รายงานวิจัยฉบับสมบูรณ์

โครงการ

ผลกระทบของการกระจายตัวและขนาดของอนุภาคขนาดนาโนเมตรของซิงก์ออกไซด์ในฟิล์มพอลิอิไมด์ที่มีต่อสมบัติการเปล่งแสง

(Effect of Degree of Dispersion and Particle Size of ZnO Nanoparticles in Polyimide Films on Light Emitting Properties)

โดย

อ.ดร. อนงค์นาฏ สมหวังธนโรจน์

ภาควิชาวิศวกรรมเคมี คณะวิศวกรรมศาสตร์

จุฬาลงกรณ์มหาวิทยาลัย

20 มิถุนายน 2551

สัญญาเลขที่ MRG4980135

รายงานวิจัยฉบับสมบูรณ์

โครงการผลกระทบของการกระจายตัวและขนาดของอนุภาคขนาดนาโนเมตรของซิงก์ออกไซด์ในฟิล์มพอลิอิไมด์ที่มีต่อสมบัติการเปล่งแสง

โดย

ดร. อนงค์นาฏ สมหวังธนโรจน์

ภาควิชาวิศวกรรมเคมี คณะวิศวกรรมศาสตร์

จุฬาลงกรณ์มหาวิทยาลัย

สนับสนุนโดยสำนักงานกองทุนสนับสนุนการวิจัย

บทคัดย่อ

รหัสโครงการ MRG4980135

ชื่อโครงการ :ผลกระทบของการกระจายตัวและขนาดของอนุภาคขนาดนาโนเมตรของซิงก์ออกไซด์ในฟิล์มพอลิอิไมด์ที่มีต่อสมบัติการเปล่งแสง

ชื่อนักวิจัย :

1. ดร. อนงค์นาฏ สมหวังธนโรจน์	ภาควิชาวิศวกรรมเคมี คณะวิศวกรรมศาสตร์ จุฬาลงกรณ์มหาวิทยาลัย
2. ศ.ดร.วิวัฒน์ ตัณฑะพานิชกุล	ศูนย์นาโนเทคโนโลยีแห่งชาติ สำนักงานพัฒนาวิทยาศาสตร์และเทคโนโลยีแห่งชาติ3.
Prof. Dr. Shinji Ando	Department of Chemistry and Materials Science Tokyo Institute of Technology

E-mail Address : anongnat.s@chula.ac.th

ระยะเวลาโครงการ : 2 ปี

งานวิจัยนี้เตรียมฟิล์มพอลิอิไมด์ที่มีซิงก์ออกไซด์ขนาดนาโนเมตรกระจายอยู่โดยทำได้สองวิธีคือ หนึ่งการเติมสารประกอบซิงก์ลงในสารละลายพอลิเอมิกแอซิดและตามด้วยปฏิกิริยาการสลายตัวทางความร้อนให้ได้ซิงก์ออกไซด์ในเนื้อพอลิเมอร์ และสองการเติมอนุภาคนาโนของซิงก์ออกไซด์ลงในพอลิเมอร์โดยตรง จากการทดลองพบว่าการเติมสารประกอบซิงก์ทั้งซิงก์ไนเตรด ($Zn(NO_3)_2$) และ zinc hexafluoroacetylacetonate (Zn(hfac)) สามารถถูกเปลี่ยนให้เป็นนาโนอนุภาคของซิงก์ออกไซด์ในเนื้อพอลิอิไมด์โดยการสลายตัวทางความร้อนขณะที่เกิดปฏิกิริยาการบ่มของพอลิอิไมด์ได้โดยสามารถยืนยันได้จากเทคนิค XRD และจากการศึกษาสมบัติทางความร้อนของฟิล์มเหล่านี้พบว่าเสถียรภาพทางความร้อนของฟิล์มสามารถเรียงได้ตามลำดับดังนี้ ฟิล์มที่ใส่ซิงก์ออกไซด์โดยตรง (ZnO/PI) > ฟิล์มที่ได้จากการใส่ Zn(hfac) (Zn(hfac/PI) > ฟิล์มที่ได้จากการใส่ซิงก์ไนเตรด ($Zn(NO_3)_2$/PI) นอกจากนี้สมบัติในการเปล่งแสงนั้นพบว่า ZnO/PI > $Zn(NO_3)_2$/PI > Zn(hfac)/PI จากภาพถ่าย TEM พบว่าอนุภาคในฟิล์ม ZnO/PI ที่ความเข้มข้นสูง (117 mol%) มีลักษณะเป็นกลุ่มก้อนที่มีขนาดเฉลี่ย 17 – 90 นาโนเมตร ซึ่งมีลักษณะการกระจายตัวทั่วเนื้อฟิล์มแต่ไม่กระจายตัวในระดับนาโนเมตร

ข้อเสนอแนะสำหรับงานวิจัยนี้คือหาสารที่ช่วยในการกระจายตัวของอนุภาคซิงก์ออกไซด์ในเนื้อพอลิเมอร์ เพื่อเพิ่มสมบัติการเปล่งแสงและความใสของเนื้อฟิล์มที่ได้

คำหลัก : พอลิอิไมด์; ซิงก์ออกไซด์; นาโนอนุภาค; ฟลูออเรสเซนส์; สมบัติเชิงความร้อน

Abstract

Project Code : MRG4980135

Project Title : Effect of Degree of Dispersion and Particle Size of ZnO Nanoparticles in Polyimide Films on Light Emitting Properties

Investigator :

1. Dr. Anongnat Somwangthanaroj — Department of Chemical Engineering, Faculty of Engineering, Chulalongkorn University
2. Prof. Dr. Wiwut Tanthapanichakoon — National Nanotechnology Center, National Science and Technology and Development Agency
3. Prof. Dr. Shinji Ando — Department of Chemistry and Materials Science Tokyo Institute of Technology

E-mail Address : anongnat.s@chula.ac.th

Project Period : 2 years

Polyimide (PI) films containing dispersed zinc oxide (ZnO) nanoparticles can be prepared from two methods; that is, adding zinc compound into poly(amic acid) solution (PAA, PI precursor), followed by thermal decomposition reaction to obtain zinc oxide in polymer matrix. The second method is to add ZnO nanoparticles directly into PAA solution. From the experiments, it was found that zinc nitrate ($Zn(NO_3)_2$) และ zinc hexafluoroacetylacetonate (Zn(hfac)) can be converted to be ZnO nanoparticles in polyimide matrix by thermal decomposition while polymer imidization occurs, which is confirmed by XRD technique. In addition, these hybrid films show the thermal stability in order as follows directly added ZnO into PI film (ZnO/PI) > thermally decomposed Zn(hfac) in PI (Zn(hfac/PI) > thermally decomposed zinc nitrate in PI ($Zn(NO_3)_2$/PI). Meanwhile, photoluminescence properties of these films are in the order as follows ZnO/PI > $Zn(NO_3)_2$/PI > Zn(hfac)/PI. From TEM images, high concentration of ZnO in ZnO/PI films (117 mol%) shows the aggregation of ZnO, whose average size is 17-90 nm, which are well distributed throughout the film but poorly dispersed in nanometer range.

Suggestion for the future study is to use the surfactant to disperse and stabilize ZnO nanoparticles in polymer matrix to enhance the photoluminescence and clarity of the film.

คำหลัก : polyimide; ZnO; nanoparticle; fluorescence; thermal properties

สารบัญ

Executive Summary

1. ความสำคัญและที่มาของปัญหา

ในงานวิจัยนี้เป็นการพัฒนาความเข้าใจและพัฒนาการทำพอลิอิไมด์ฟิล์มซึ่งมีซิงก์ออกไซด์ขนาดนาโนเมตรกระจายอย่างสม่ำเสมออยู่ โดยวัสดุนี้มีศักยภาพที่จะนำไปใช้ในวัสดุเปล่งแสง พร้อมทั้งมีสมบัติการกันรังสียูวี มีเสถียรภาพทางความร้อนสูง และเป็นฟิล์มที่โปร่งใสมาก พอลิอิไมด์ (polyimide) มีความแข็งแรงสูง มีสมบัติในการทนความร้อนและสารเคมีดีเยี่ยม และสมบัติเชิงไฟฟ้าดีมาก ทำให้มีการนำมาใช้แทนสารอนินทรีย์จำพวกแก้วและโลหะในอุตสาหกรรมหลายประเภทเช่นอิเลคทรอนิกส์ และยานอวกาศ นอกจากนี้ยังสามารถที่จะถูกใช้เป็น optical waveguide ในงานโทรคมนาคมและเทคโนโลยีการสื่อสารโดยแสง (optical interconnect technology) เนื่องจากสมบัติเชิงความร้อนและเชิงแสงที่ดีเยี่ยมของวัสดุ นอกจากนี้ยังเป็นวัสดุที่สามารถใช้เป็น short-wavelength light-emitting diodes (LEDs) และ diode lasers ซึ่งเป็นวัสดุที่มีความต้องการมากในการแสดงภาพ (display) การเปล่งแสง (illumination) และการเก็บข้อมูล (information storage)

นอกจากนี้ซิงก์ออกไซด์ (zinc oxide, ZnO) เป็นสารกึ่งตัวนำที่มีประโยชน์มากเนื่องจากมีพลังงาน exciton binding สูง ซึ่งถูกแสดงโดยการเปล่งแสงออกมาอย่างมีประสิทธิภาพเมื่อมีการกระตุ้นด้วยแสง ถ้าผลึกซิงก์ออกไซด์ที่เปล่งแสงได้โดยมีอนุภาคขนาดนาโนเมตรกระจายตัวอย่างสม่ำเสมอในวัสดุพื้น (matrix) ที่ยืดหยุ่นได้ วัสดุชนิดใหม่นี้จะมีประโยชน์มากและมีสมบัติเชิงแสงที่เฉพาะตัวซึ่งมีแนวโน้มที่จะถูกใช้ในอุตสาหกรรมเทคโนโลยีทางภาพ (visual technology) และการแสดงภาพ (display industry) เนื่องจากในปัจจุบันวัสดุเปล่งแสงที่ใช้ในผลิตภัณฑ์ต่าง ๆ ทั้ง LED (light emitting diode) และผลิตภัณฑ์ในเทคโนโลยีทางภาพอื่น ๆ ยังมักเป็นสารอนินทรีย์ซึ่งไม่มีความยืดหยุ่น ทำให้วัสดุชนิดใหม่นี้สามารถที่จะถูกนำมาใช้ในงานได้หลากหลายมากขึ้น

2. วัตถุประสงค์

โครงการนี้ศึกษาผลกระทบของขนาดและการกระจายตัวของอนุภาคขนาดนาโนเมตรของซิงก์ออกไซด์ในฟิล์มพอลิอิไมด์ที่มีต่อสมบัติในการเปล่งแสง โดยในงานวิจัยนี้จะมีการเปรียบเทียบขนาดและการกระจายตัวของอนุภาคเมื่อมีการเปลี่ยนวิธีการเตรียมฟิล์มพอลิอิไมด์ที่มีนาโนอนุภาคของซิงก์ออกไซด์อยู่ ทั้งนี้เพื่อการพัฒนาวัสดุเปล่งแสงที่มีประสิทธิภาพสูง และสามารถลดต้นทุนในการผลิต

3. ระเบียบวิธีวิจัย

3.1 รวบรวมข้อมูลของเอกสารที่เกี่ยวข้อง (literature review) และเตรียมสารเคมี อุปกรณ์ที่เกี่ยวข้อง

3.2 จัดซื้อมอนอเมอร์ และนำมาทำให้บริสุทธิ์ และทำให้แห้ง

3.3 เตรียมสารละลายพอลิเอมิดแอซิด (poly(amic acid), precursor ของพอลิอิไมด์) โดยผสมมอนอเมอร์ต่าง ๆ เข้าด้วยกันในอัตราส่วน 1:1 โดยโมล ภายใน glove box เพื่อไม่ให้มอนอเมอร์สัมผัสกับออกซิเจนและความชื้น ในงานวิจัยนี้จะมีการเลือกใช้มอนอเมอร์ 4 ชนิด เพื่อหาชนิดที่ทำให้การเปล่งแสงของอนุภาคซิงก์ออกไซด์ทำได้อย่างมีประสิทธิภาพ โดยมอนอเมอร์ที่มีหมู่ dianhydride ที่ใช้ในงานวิจัยนี้คือ 4,4'-(hexafluoroisopropyllidene)diphthalic anhydride (6FDA) เป็นมอนอเมอร์ที่มีฟลูออรีนในโครงสร้างโมเลกุล และมอนอเมอร์ที่มีหมู่ diamine ที่ถูกเลือกมาใช้ในงานวิจัยนี้มี 3 ชนิดคือ 2,2'-bis(trifluoromethyl)-4,4'-diaminobiphenyl (TFDB), 4,4'-Diaminodiphenyl Ether (ODA) และ 4,4'-Methylenebis(cyclohexylamine) (DCHM) ซึ่งการเลือกใช้มอนอเมอร์ 3 ชนิดนี้เนื่องจากมอนอเมอร์แต่ละชนิดมีสูตรโครงสร้างโมเลกุลต่างกัน ทำให้พฤติกรรมการเปล่งแสงเมื่อถูกกระตุ้นด้วยแสงยูวีต่างกัน

3.4 เตรียมสารละลายพอลิเอมิดแอซิดที่มีสารประกอบซิงก์กระจายตัวอยู่โดยการเตรียมสารละลายนี้จะปรับเปลี่ยนวิธีการใส่ซิงก์ออกไซด์ 2 วิธีและเปรียบเทียบผลนั่นคือ

1. ใช้วิธีการสลายตัวของสารประกอบซิงก์ หรือเกลือของซิงก์ ให้ได้ซิงก์ออกไซด์ขณะบ่มฟิล์มพอลิเอมิก แอซิดในตู้อบความร้อนสูงเพื่อให้เกิดปฏิกิริยาอิมิไดเซชั่น (Imidization) และเปลี่ยนเป็นฟิล์มพอลิอิไมด์ ซึ่งในงานวิจัยนี้ได้เลือกใช้ Zinc hexafluoroacetylacetonate dehydrate (Zn(hfac)), Zinc acetylactonate hydrate (Zn(ac) และ Zinc Nitrate Hexahydrate (Zn(Ni)) เป็นสารตั้งต้นซิงก์ โดยผู้เสนอขอทุนได้ทดลองเบื้องต้นขณะทำวิจัยที่ญี่ปุ่นกับอาจารย์ Ando และสามารถทำให้สารประกอบเหล่านี้เปลี่ยนเป็นนาโนอนุภาคซิงก์ออกไซด์ได้ในขณะบ่มฟิล์มสารละลายพอลิเอมิก แอซิดให้ได้ฟิล์มพอลิอิไมด์ออกมา

2. ใส่อนุภาคขนาดนาโนเมตรของซิงก์ออกไซด์ (ที่จัดซื้อมา) ลงในสารละลายพอลิเอมิดแอซิด โดยใส่ stabilizer (ในงานวิจัยนี้เลือกใช้สาร 3-[Tris(trimethylsiloxy)silyl]propyl methacrylate (TPM) เป็น stabilizer) ลงไปพร้อมกันเพื่อให้ซิงก์ออกไซด์กระจายตัวได้ดี (จากนั้นทำการทดสอบเวลาที่อนุภาคสามารถกระจายตัวและแขวนลอยอยู่ในสารละลายพอลิเอมิก แอซิดก่อน เพื่อจะทำให้รู้ว่า stabilizer ชนิดที่เลือกมา ทำหน้าที่ได้ดี และอนุภาคสามารถแขวนลอยอยู่ได้นานพอที่สารละลายพอลิเอมิก แอซิด จะถูกบ่มเปลี่ยนเป็นฟิล์มแข็งของพอลิอิไมด์ได้โดยนาโนอนุภาคไม่เกาะกลุ่มกัน และเมื่อฟิล์มเป็นของแข็ง นาโนอนุภาคของซิงก์ออกไซด์จะถูกตรึงไว้โดยฟิล์ม)

3.5 เตรียมฟิล์มพอลิอิไมด์ที่มีอนุภาคขนาดนาโนเมตรของซิงก์ออกไซด์กระจายตัวอยู่โดย

1. หยดสารละลายพอลิเอมิดแอซิดลงบนแผ่นซิลิกอนซึ่งวางบนเครื่อง spin coater ที่ตั้งอยู่ในบริเวณที่ปลอดฝุ่น เพื่อไม่ให้สิ่งแปลกปลอมตกลงบนฟิล์ม ทำให้สมบัติเชิงแสงของฟิล์มเปลี่ยนไป

2. ตั้งค่าความเร็วในการหมุนของเครื่องเพื่อให้ได้ความหนาของฟิล์มที่สม่ำเสมอและสามารถควบคุมความหนาของฟิล์มได้ด้วยความเร็วรอบและเวลาในการหมุน

3. นำฟิล์มที่ได้พร้อมแผ่นซิลิกอนไปบ่มโดยปรับเปลี่ยนสภาวะต่าง ๆ (อุณหภูมิ, ก๊าซในตู้อบ และเวลาในการบ่ม) เพื่อให้สารประกอบซิงก์เปลี่ยนเป็นซิงก์ออกไซด์ที่เปล่งแสงได้

ประสิทธิภาพสูงสุด จะได้ฟิล์มพอลิอิไมด์ซึ่งมีอนุภาคขนาดนาโนเมตรของซิงก์ออกไซด์กระจายตัวอยู่

3.6 ทดสอบสมบัติของฟิล์มที่เตรียมได้ โดยศึกษาสมบัติในการเปล่งแสง สมบัติเชิงกล เชิงความร้อน การเปลี่ยนแปลงโครงสร้างของหมู่ฟังก์ชันของ stabilizer และศึกษาขนาด, การกระจายตัว และลักษณะของซิงก์ออกไซด์

3.7 วิเคราะห์ข้อมูล จัดทำรายงาน นำเสนอผลงาน

4. แผนการดำเนินงานวิจัยตลอดโครงการในแต่ละช่วง 6 เดือน

กิจกรรม	ไตรมาส1	ไตรมาส2	ไตรมาส3	ไตรมาส4	ไตรมาส5	ไตรมาส6	ไตรมาส7	ไตรมาส8
รวบรวมข้อมูลวิจัยที่เกี่ยวข้อง	■							
เตรียมอุปกรณ์และสารเคมี	■							
เตรียมพอลิเอมิด แอซิด (PAA)		■						
เตรียมฟิล์มโดยใส่สารประกอบซิงก์		■	■	■				
เตรียมฟิล์มโดยใส่อนุภาคขนาดนาโนเมตรของ ZnO และ stabilizer					■	■	■	
วิเคราะห์สมบัติของซิงก์ออกไซด์และฟิล์ม			■	■	■	■	■	
สรุปผลและจัดทำรายงาน								■

5. ผลงาน/หัวข้อเรื่องที่คาดว่าจะตีพิมพ์ในวารสารวิชาการระดับนานาชาติในแต่ละปี

ปีที่ 1 ชื่อเรื่องที่คาดว่าจะตีพิมพ์ Effect of zinc precursor on thermal and light emission properties of ZnO nanoparticles embedded in polyimide films via thermal decomposition process

ชื่อวารสารที่คาดว่าจะตีพิมพ์ Journal of Materials Research (impact factor : 1.912)

ปีที่ 2 ชื่อเรื่องที่คาดว่าจะตีพิมพ์ Effect of the origin of ZnO Nanoparticles Dispersed in Polyimide Films on their Photoluminescence and Thermal Stabilit

ชื่อวารสารที่คาดว่าจะตีพิมพ์ Journal of Applied Polymer Science (impact factor : 1.306)

เนื้อหางานวิจัย

งานวิจัยในโครงการนี้จะแบ่งออกเป็น 2 ส่วนคือ
ส่วนที่ 1 จะศึกษาผลกระทบของชนิดของสารประกอบซิงก์ที่มีผลต่อการเกิดซิงก์ออกไซด์ในเนื้อพอลิอิไมด์ฟิล์มโดยวิธีการสลายตัวทางความร้อนขณะเกิดปฏิกิริยาการบ่มพอลิอิไมด์

ส่วนที่ 2 จะศึกษาเปรียบเทียบผลกระทบของนาโนอนุภาคซิงก์ออกไซด์ที่มีต่อสมบัติเชิงความร้อนและการเปล่งแสงของฟิล์มพอลิอิไมด์ที่มีซิงก์ออกไซด์กระจายตัวอยู่

ส่วนที่ 1

Effect of zinc precursor on thermal and light emission properties of ZnO nanoparticles embedded in polyimide films via thermal decomposition process

A. Anongnat Somwangthanaroj[*,a], K. Suwanchatchai[a], S. Ando[b], W. Tanthapanichakoon[c]

[a] Department of Chemical Engineering, Faculty of Engineering, Chulalongkorn University, Bangkok 10330, Thailand

[b] Department of Chemistry and Materials Science, Tokyo Institute of Technology, Tokyo 152-8552, Japan

[c] National Nanotechnology Center, National Science and Technology Development Agency, Pathumtani 12120, Thailand

Abstract

A novel nanocomposites consisting of fluorinated polyimide (PI) films and zinc oxide (ZnO) nanoparticles, from which green light emission is observed, have successfully been prepared. The embedded ZnO nanoparticles in PI films are prepared by adding two separate zinc compounds in poly(amic acid) (PAA) solution followed by thermal curing to convert PAA to PI. The added zinc hexafluoroacetylacetonate dihydrate (Zn(hfac)) and zinc nitrate hexahydrate ($Zn(NO_3)_2$), are converted by thermal decomposition to semicrystalline ZnO nanoparticles, which is confirmed by XRD technique. The green light emission of the nanocomposite films irradiated by UV light is caused by the intrinsic defects in ZnO crystallites. The PI films embedded with ZnO from $Zn(NO_3)_2$ emits much higher fluorescent intensity than their counterparts from Zn(hfac). In addition, the Zn(hfac)/PI film is thermally more stable than the $Zn(NO_3)_2$/PI one. From TEM images, the size of ZnO nanoparticles in PI films derived from 28 mol% Zn(hfac) is much larger than those from 59 mol% $Zn(NO_3)_2$.

Keywords: A. Nano composite; A. Polymer-matrix composites (PMCs); B. Thermal properties; luminescence

* To whom all correspondence should be addressed

Email: anongnat.s@chula.ac.th

Phone: 662-218-6864 Fax: 662-218-6877

1. Introduction

Polyimide (PI) provides strong, astoundingly thermal and chemical resistance, high thermoxidative stability, high modulus and excellent electrical properties, but it lacks sufficient properties required for optical light-emitting applications. Therefore, new kinds of PI have been developed [1]. One approach is to add fluorine atoms in the skeletal structures of PIs which modifies several properties such as radiation durability against UV light, transparency in the visible and NIR regions, lower the glass transition temperature and increase thermal expansion coefficient. As a result of these exceptional thermal and optical properties, the fluorinated PI has potential as optical waveguides in telecommunication and optical interconnect technologies.

Zinc oxide (ZnO) is an *n*-type semiconductor, which has a band gap of 3.4 eV and a large exciton binding energy of 60 meV. Violet electroluminescence is observed for specially prepared ZnO at room-temperature, and blue LED is successfully demonstrated [2]. ZnO nanoparticles can be deposited directly onto PI film by pulse laser deposition [3, 4] or by using a stabilizer to prevent aggregation of directly added ZnO nanoparticles [5-7]. In addition, PI films containing metal oxide nanoparticles can be prepared by embedding thin metal film on a quartz substrate, coating them with poly(amic acid) (PAA) solution and thermal curing the materials [8]. The PI films containing ZnO nanoparticles show a broad absorption peak around 374 nm corresponding to exciton absorption; therefore, the optical band edge would be above 370 nm which is close to the bulk value [9]. It is reported that the uniform dispersion of metal or metal oxide nanoparticles in PIs improves their radiation durability, transparency, refractive indices and birefringence properties [10].

In contrast to the aforementioned methods, this study proposes a novel *in-situ* thermal decomposition method to synthesize ZnO nanoparticles embedded in PI films. Metallic nanoparticle dispersed in fluorinated PI films is prepared by thermal curing of PAAs containing metallic salts or organometallic complexes, which are subsequently decomposed to yield either zero-valent metal or metal oxides via thermal curing process [11].

In this study PI films embedded with uniformly dispersed ZnO nanoparticles are prepared following Sawada and Ando's method [11]. More specifically, the zinc complex or zinc salt of interest is dispersed in PAA solution and decomposed during the thermal imidization process. The main focus of this investigation is to develop a better

understanding and a promising way of creating a new series of PI films embedded with uniformly dispersed ZnO nanoparticles. These highly transparent films have high potential for optical light-emitting applications together with UV-resistance.

2. Materials and methods

Materials

The fluorinated polyimide used in this study is synthesized from 4,4'-(hexafluoroisopropyllidene) diphthalic anhydride (6FDA) and 2,2'-bis(trifluoromethyl)-4,4'-hexafluoropropane diaminobiphenyl (TFDB) as shown in Figure 1. Monomers are purified by sublimation process before use. In this process, the dianhydride and diamine react in a dipolar aprotic solvent *N,N*-dimethylacetamide (DMAc) obtained from Aldrich Chemical Co. Zinc nitrate hexahydrate ($Zn(NO_3)_2 \cdot 6H_2O$) (99.9% purity) and zinc hexafluoroacetylacetonate dehydrate (Zn(hfac)) (98% purity) are also obtained from Aldrich Chemical Co and are used as received.

Preparation of poly(amic acid) solution

As shown in Figure 1, 6FDA/TFDB-PI is prepared by the reaction between 6FDA and TFDB, which have six fluorine atoms in both monomers. More specifically, TFDB is completely dissolved in *N,N*-dimethylacetamide (DMAc) solvent to give a clear, colorless solution. Then an equimolar amount of 6FDA is slowly added to the solution with stirring to obtain a 15 wt% poly(amic acid) (PAA) solution. The solution is gently stirred at room temperature for 24 h. Poly(amic acid), which contains carboxamide and carboxyl group is obtained from the reaction between dianhydride from 6FDA with diamine from TFDB as shown in Figure 1. The detailed preparation of poly(amic acid) (PAA), the precursor of the polyimide, and the thermal, mechanical, and chemical properties of this polyimide have been described elsewhere.[1]

Preparation of the ZnO/PI films

5 – 59 mol% of either $Zn(NO_3)_2 \cdot 6H_2O$ or Zn(hfac) is added into the above PAA solution at the desired molar concentration of ZnO and stirred overnight. Note that the concentration of ZnO in PI films is expressed as a percentage by mole of the ZnO comparing to the repeating unit of PI. All the synthesizing and mixing procedures are performed in nitrogen atmosphere. The PAA solution is then spin-cast onto a clean dry silicon substrate to obtain a thin layer of solution of uniform thickness. The PAA layer is then cured at 350 ~ 390ºC in nitrogen atmosphere or in vacuo according to the following

steps: 70ºC, 30 min, ramp up to 350ºC in 1 h and isothermal at 350 ~ 390ºC for 1 h. The heat treatment promotes dehydration and ring closure, which converted PAA to polyimide. In this study, the PI films containing nanoparticles of ZnO obtained from thermal decomposition of Zn(hfac) and $Zn(NO_3)_2$ are designated as Zn(hfac)/PI and $Zn(NO_3)_2$/PI, respectively.

Measurements

Nanoparticle ZnO/PI films and pure PI film (6 – 20 μm thickness) are characterized by wide-angle X-ray diffraction (XRD) at ambient temperature on X'Pert-MPD (PANalytical, Netherlands) with CuK_α radiation of wavelength 1.54 Å. Thermogravimetric analysis (TGA, TA Instruments SDT Q-600) is used to determine the degradation temperature at heating rate 20 °C·min^{-1} from 35 to 1000°C under nitrogen atmosphere. The transmission and reflectance spectra in the visible and near-infrared regions (Vis-NIR, λ = 200 – 2000 nm) of the PI films on substrate are measured using a U-3500 spectrophotometer (Hitachi, Japan). Photoluminescence (PL) scans are carried out with a fluorescence spectrophotometer F-4500 (Hitachi, Japan). Three-dimensional contour plots provided the maximum spectral information. Cross-sectional transmission electron (TEM) micrographs of ZnO-doped PIs are taken with TEM 200CX (JEOL, Japan). The PI films are embedded in epoxy resin and sectioned into a thickness of 60 nm with a Reichert-Jung Werke ultramicrotome.

3. Results and discussion

The XRD characterization results are depicted in Figure 2. The XRD peaks, which correspond to the {100}, {002}, {101}, {110} and {103} basal diffraction of ZnO, are indicative of crystal structure of ZnO nanoparticles [12, 13]. The 6FDA-TFDB polyimide (PI) film prepared from a PAA containing 28 mol% of Zn(hfac) shows the most distinct peaks indicating the existence of ZnO crystal structure in the polyimide film. Though the 59 mol% $Zn(NO_3)_2$/PI film shows broad peaks with low intensity, it is confirmed that $Zn(NO_3)_2$ dissolved in PAA solution is successfully converted to ZnO nanoparticles by thermal decomposition. However, the 5, 10 and 15 mol% $Zn(NO_3)_2$/PI film do not show any XRD peaks because the nanoparticles precipitated in the other samples are supposed to be too small in size or they possess only imperfect crystalline structures and too little amount of ZnO below the detection limit of the diffractometer which is consistent with the report of Sawada and Ando [11] and Chiang and Wang[14]. Only the selected XRD patterns showed here exhibit the crystal structure of ZnO.

For thermal stability characteristics of nanocomposite films, the presence of ZnO nanoparticles in PI films affects the degradation temperature (T_d), which is defined as the temperature of the samples at 5 wt% loss, of ZnO/PI film. It is found that the T_d of $Zn(NO_3)_2$/PI are lower than those of Zn(hfac)/PI. Figure 3a shows the thermogravimetric profiles of Zn(hfac)/PI films. The T_d of these hybrid films decrease when adding Zn(hfac) nanoparticles directly into the films. Addition of 5 to 20 mol% of Zn(hfac) into PI films decrease the T_d by 24 ^{o}C to 97 ^{o}C. Furthermore, figure 3b shows the thermogravimetric profiles of $Zn(NO_3)_2$/PI films. As can be seen, the addition of 5 mol% of $Zn(NO_3)_2$ into PI films decrease the T_d of hybrid films compared to the pure PI. However, adding more amounts of $Zn(NO_3)_2$/PI from 5 to 20 mol% decrease the T_d by 61 ^{o}C to 107 ^{o}C. Interestingly, the Zn(hfac)/PI and $Zn(NO_3)_2$/PI films prepared at the same concentration but show the different thermogravimetric profiles. For example, at 15 mol% of ZnO content, the T_d of Zn(hfac)/PI decrease only by 54 ^{o}C compared to 102 ^{o}C in the case of $Zn(NO_3)_2$/PI. Obviously the Zn(hfac)/PI film has better thermal stability than the $Zn(NO_3)_2$/PI film. The difference between the T_d of Zn(hfac)/PI and that of $Zn(NO_3)_2$/PI film is caused by the origin of ZnO nanoparticles. Since metallic salts added into PI films induced oxidative degradation of polyimide, the T_d of $Zn(NO_3)_2$/PI film decreases dramatically[11, 14]. This result is consistent with Hsu et al's[6] and Chiang and Whang's[14].

ZnO is widely used as inorganic fillers but also known as a wide band gap semiconducting material, which has potential uses in optical applications. By introducing ZnO nanoparticles in the PI matrix, ZnO/PI nanocomposite with controlled properties could be expected. The fluorescence spectra observed for the pure PI films and PI containing 5 mol% ZnO nanoparticles from Zn(hfac) are shown in Figure 4. By adding only 5 mol% of Zn(hfac) into PAA solution, followed by thermal cure to obtain Zn(hfac)/PI film, fluorescence emission at visible wavelength is enhanced by 6 times compared to that of its matrix. The emission peak is also shown red-shift, i.e., fluorescence emission is shifted from 491.2 nm to 497.6 nm with ZnO containing in PI film. Note that the intensity of fluorescence emission from excitation wavelength in the range of 300 nm does not change because these fluorescence emissions come from polyimide matrix.

The effects of ZnO concentration from Zn(hfac) and $Zn(NO_3)_2$, respectively, in PI film on the fluorescence and absorbance are presented in Figures 5a and 5b. As expected, the existence of ZnO in PI films enhances the fluorescence emission. By adding

only 5 mol% of ZnO from either Zn(hfac) or $Zn(NO_3)_2$ into PI film, fluorescence emission intensity at the visible wavelength 497.6 nm, which is excited at 417 nm for Zn(hfac)/PI, and 488.8 nm, which is excited at 406.8 nm for $Zn(NO_3)_2$/PI) is 6.0 and 18.4 times higher than that of pure PI film, respectively. In fact, emission spectra of both nanocomposites and pure PI films excited at around 300 nm are approximately the same in both wavelength and intensity (data not shown). Therefore, the excitation wavelength of ~ 410 nm is suitable for nanocomposite films to exhibit green light emission. Furthermore, the emission peak of $Zn(NO_3)_2$/PI film is displaced to shorter wavelength (hypsochromic shift) with much higher intensity than that of Zn(hfac)/PI film, whereas the emission peaks of the former are 3.1 times of those of the latter. The visible light emission of ZnO is caused by oxygen vacancy and interstitial zinc of ZnO [15-17]. Note that no XRD peak is observed from 5 mol% $Zn(NO_3)_2$/PI films. Since visible emission could not be obtained from amorphous ZnO, the visible emission from this film, which dominates the photoluminescence (PL) spectra, should come from an imperfect crystal structure or excessively small size of ZnO nanoparticles [18].

As the concentration of ZnO nanoparticles from Zn(hfac) increases from 0 to 28 mol%, figure 5a shows that all samples exhibited absorption spectra in the range of 300 – 370 nm. Above 370 nm, only the absorbance of pure PI was quenched in the visible region. As the concentration of ZnO nanoparticles from Zn(hfac) increases from 5 to 28 mol%, the fluorescent intensity decreases from 6.0 to 4.3 times compared to that of pure PI, although the wavelength of the excitation peak of all films is approximately the same. The fluorescence could be absorbed by the other molecules. This is consistent with the appearance of an increase in the absorption in the visible region (above 370 nm).

Similarly, the effects of ZnO concentration from thermal decomposition of $Zn(NO_3)_2$ in PI films on the absorbance and fluorescence of $Zn(NO_3)_2$/PI films are shown in Figures 5b. $Zn(NO_3)_2$/PI films of all concentrations exhibit broad absorption in the range of 300 – 370 nm. The absorption above 370 nm gradually increase as the concentration of $Zn(NO_3)_2$ increase. Adding only 5 mol% of $Zn(NO_3)_2$ to the PI film shows 18.4 times higher intensity in the visible region that pure PI film. In addition, the intensities of 10, 15 and 59 mol% Zn $(NO_3)_2$/PI are 20.9, 21.6 and 5.1 times of that of pure PI film. The fluorescence emission intensity of 59 mol% $Zn(NO_3)_2$ decreases owing to the aggregation of ZnO nanoparticles (confirmed by TEM). Moreover, the emission peak of 59 mol% $Zn(NO_3)_2$/PI films was red shifted when compared to those of the other hybrid films, which may also be

attributed to the aggregation of ZnO nanoparticles. This result is consistent with the appearance of the increasing absorption above 370 nm. In addition, the light emission of Zn(hfac)/PI films are also red shifted compared to that of pure PI. This phenomenon could be explained by the quantum confinement mechanism and interactions between the oxygens of ZnO and functional groups in PI.

Figure 6 shows the TEM micrographs, respectively, of 28 mol% Zn(hfac) and 59 mol% $Zn(NO_3)_2$ in 6FDA-TFDB polyimide matrix. The size of ZnO nanoparticles derived from 28 mol% Zn(hfac) is much larger than those from 59 mol% $Zn(NO_3)_2$. These smaller ZnO nanoparticles from $Zn(NO_3)_2$ gives rise to higher fluorescent emission intensity than the bigger ZnO nanoparticles from Zn(hfac) (from photoluminescence data). Note that no ZnO nanoparticles are observable in the TEM micrographs of the other ZnO/PI films in this study possibly due to the limitation of TEM resolution.

4. Conclusions

In this study, $Zn(NO_3)_2$/PI films emits stronger green fluorescence and yields smaller ZnO nanoparticles dispersed thoroughly in the film. The introduction of 15 mol% of $Zn(NO_3)$ in PI would be the optimal concentration to give high fluorescent intensity. However, $Zn(NO_3)_2$/PI films are thermally less stable than the Zn(hfac)/PI ones. In addition, only broad typical patterns of ZnO crystallites are observed in the XRD and TEM for high concentration of both Zn(hfac) and $Zn(NO_3)_2$ added into PAA solution due to the very small particle sizes and low degree of crystallization of ZnO nanoparticles, though the distinct green-light fluorescence originating from ZnO are observed around 480-490 nm.

Acknowledgements

The authors acknowledge financial support from Thailand Research Fund (TRF) and Thailand-Japan Technology Transfer Project (TJTTP) and thank the Center for Advanced Materials Analysis, Tokyo Institute of Technology, for TEM images.

References

[1] Matsuura T, Hasuda Y, Nishi S, Yamada Y. Polyimide derived from 2,2'-bis(trifluoromethyl)-4,4'-diaminobiphenyl. 1. Synthesis and characterization of polyimides prepared with 2,2'-bis(3,4-dicarboxyphenyl)hexafluoropropane dianhydride or pyromellitic dianhydride. Macromol 1991;24(18)5001-5005.

[2] Tsukazaki A, Ohtomo A, Onuma T, Ohtani M, Makino T, Sumiya M, Ohtani K, Chichibu SF, Fuke S, Segawa Y, Ohno H, Koinuma H, Kawasaki M. Repeated temperature modulation epitaxy for p-type doping and light-emitting diode based on ZnO. Nat. Mater 2005;4(1)42-46.

[3] Matsumura M, Camata RP. Pulsed laser deposition and photoluminescence measurements of ZnO thin films on flexible polyimide substrates. Thin Solid Films 2005;476(2)317-321.

[4] Suh KJ, Okada H, Wakahara A, Kim HJ, Chang HJ, Yoshida A Transparent conducting ZnO films on polymer substrates by pulsed laser deposition. 1-3, 2004.

[5] Guo ZH, Wei SY, Shedd B, Scaffaro R, Pereira T, Hahn HT. Particle surface engineering effect on the mechanical, optical and photoluminescent properties of ZnO/vinyl-ester resin nanocomposites. Journal of Materials Chemistry 2007;17(8)806-813.

[6] Hsu SC, Whang WT, Hung CH, Chiang PC, Hsiao KN. Effect of the polyimide structure and ZnO concentration on the morphology and characteristics of polyimide/ZnO nanohybrid films. Macromolecular Chemistry and Physics 2005;206(2)291-298.

[7] Hung CH, Whang WT. Effect of surface stabilization of nanoparticles on luminescent characteristics in ZnO/poly(hydroxyethyl methacrylate) nanohybrid films. J. Mater. Chem 2005;15267-274.

[8] Chung Y, Park HP, Jeon HJ, Yoon CS, Lim SK, Kim YH. Synthesis of oxide nanoparticies embedded in polyimide. J Vac Sci Technol B 2003;21(6)L9-L11.

[9] Wu HZ, Qiu DJ, Cai YJ, Xu XL, Chen NB. Optical studies of ZnO quantum dots grown on Si(001). Journal of Crystal Growth 2002;245(1)50-55.

[10] Matsuura T, Ando S, Sasaki S, Yamamoto F. Polyimides Derived from 2,2'-Bis(Trifluoromethyl)-4,4'-Diaminobiphenyl .4. Optical-Properties of Fluorinated Polyimides for Optoelectronic Components. Macromol 1994;27(22)6665-6670.

[11] Sawada T, Ando S. Synthesis, characterization, and optical properties of metal-containing fluorinated polyimide films. Chem. Mater 1998;10(11)3368-3378.

[12] Banerjee D, Lao JY, Wang DZ, Huang JY, Ren ZF, Steeves D, Kimball B, Sennett M. Large-quantity free-standing ZnO nanowires. Appl Phys Lett 2003;83(10)2061-2063.

[13] Cho S, Ma J, Kim Y, Sun Y, Wong GKL, Ketterson JB. Photoluminescence and ultraviolet lasing of polycrystalline ZnO thin films prepared by the oxidation of the metallic Zn. Appl Phys Lett 1999;75(18)2761-2763.

[14] Chiang PC, Whang WT. The synthesis and morphology characteristic study of BAO-ODPA polyimide/TiO_2 nano hybrid films. Polymer 2003;44(8)2249-2254

[15] Lin B, Fu Z, Jia Y. Green luminescent center in undoped zinc oxide films deposited on silicon substrates. Appl. Phys. Lett 2001;79943-945.

[16] Lin Y, Xie J, Wang H, Li Y, Chavez C, Lee SY, Foltyn SR, Crooker SA, Burrell AK, McCleskey TM, Jia QX. Green luminescent zinc oxide films prepared by polymer-assisted deposition with rapid thermal process. Thin Solid Films 2005;492101-104.

[17] Masuda Y, Kinoshita N, Sato F, Koumoto K. Site-selective deposition and morphology control of UV-and visible-light-emitting ZnO crystals. Cryst. Growth. Des 2006;6(1)75-78.

[18] Wang ZJ, Wang ZJ, Zhang LG, Yuan JS, Yan SG, Wang CY. Room - temperature dual excitonic emission from amorphous ZnO. Chin Phys Lett 2003;20(5)696-699.

Figure captions

Figure 1. Preparation process of poly(amic acid) and polyimide

Figure 2. XRD patterns of pure 6FDA-TFDB polyimide film. PI containing ZnO nanoparticles from thermal decomposition of $Zn(NO_3)_2$ hexahydrate and Zn(hfac)

Figure 3. Thermogravimetric profiles of PI containing ZnO nanoparticles from thermal decomposition of (a) Zn(hfac) (b) $Zn(NO_3)_2$ hexahydrate.

Figure 4. Comparison of photoluminescence between pure PI and 5 mol% Zn(hfac) in polyimide films

Figure 5. Effect of ZnO concentration on absorbance and fluorescence of (a) Zn(hfac)/PI films and (b) $Zn(NO_3)_2$/PI films

Figure 6. TEM micrographs of ZnO in PI film (a) 28 mol% Zn(hfac)/PI (2.94 wt% ZnO) (b) 59.7 mol% $Zn(NO_3)_2$/PI (6.26 wt% ZnO)

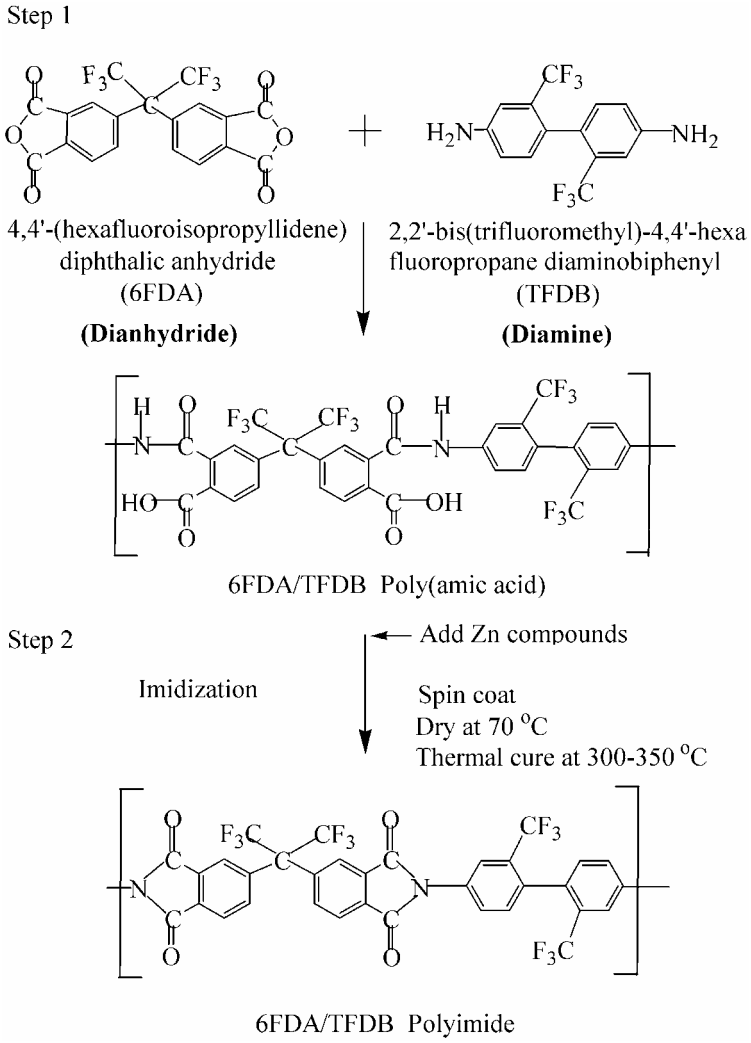
Step 1
4,4'-(hexafluoroisopropyllidene) diphthalic anhydride (6FDA)
(Dianhydride)
2,2'-bis(trifluoromethyl)-4,4'-hexa fluoropropane diaminobiphenyl (TFDB)
(Diamine)
6FDA/TFDB Poly(amic acid)
Step 2
Add Zn compounds
Imidization
Spin coat
Dry at 70 °C
Thermal cure at 300-350 °C
6FDA/TFDB Polyimide

Figure 1.

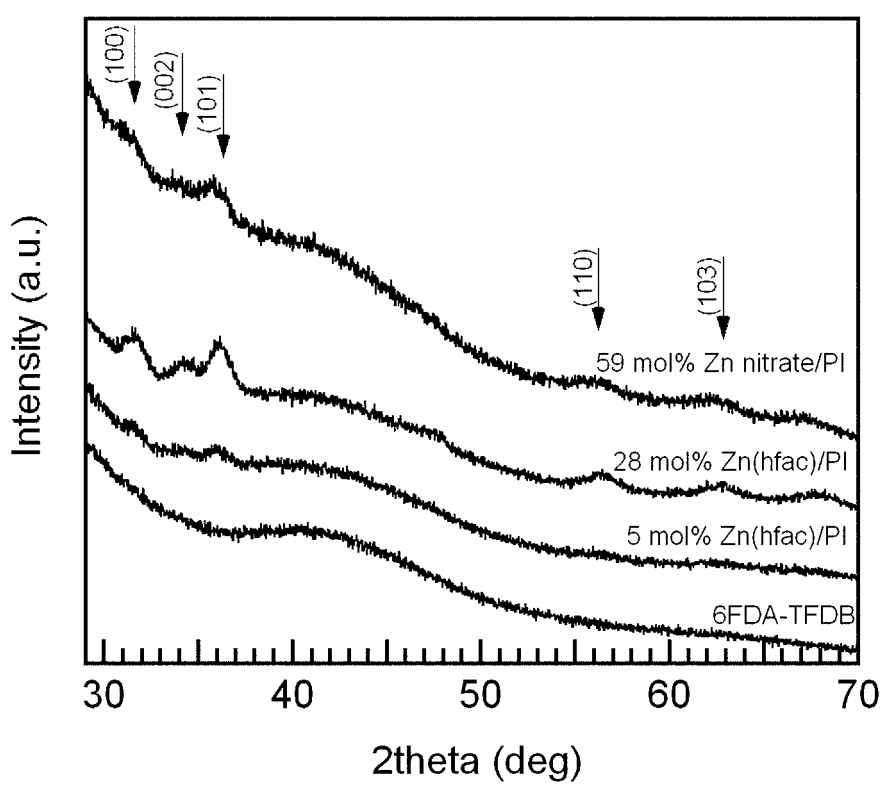

Figure 2.

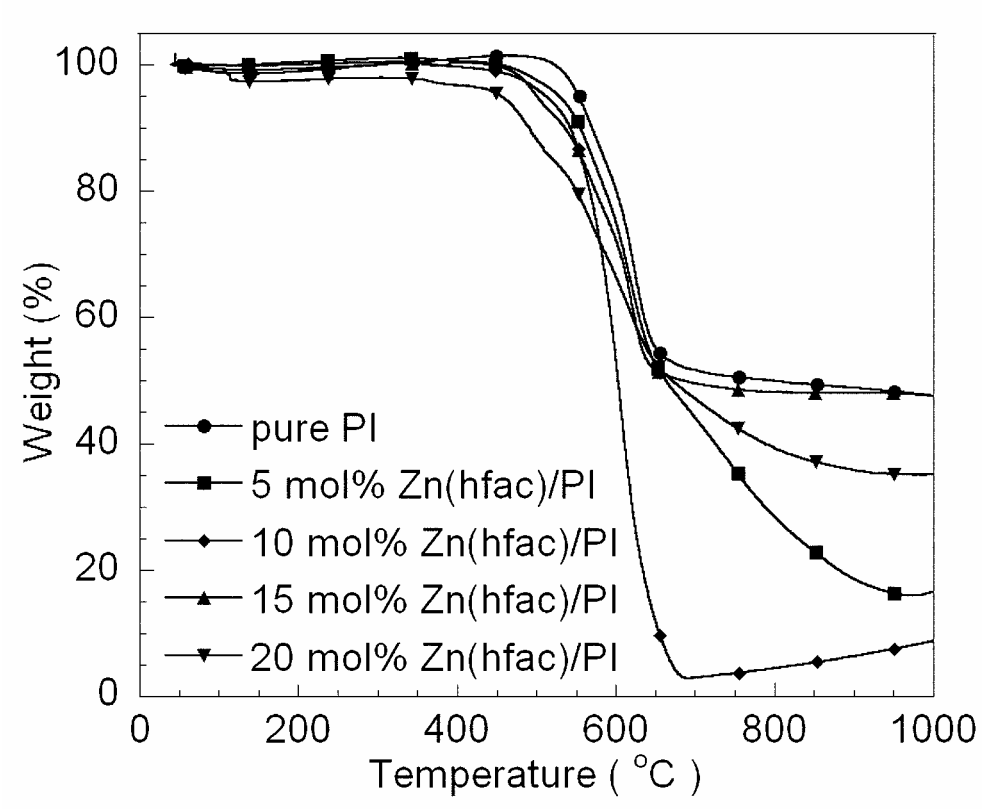

Figure 3a.

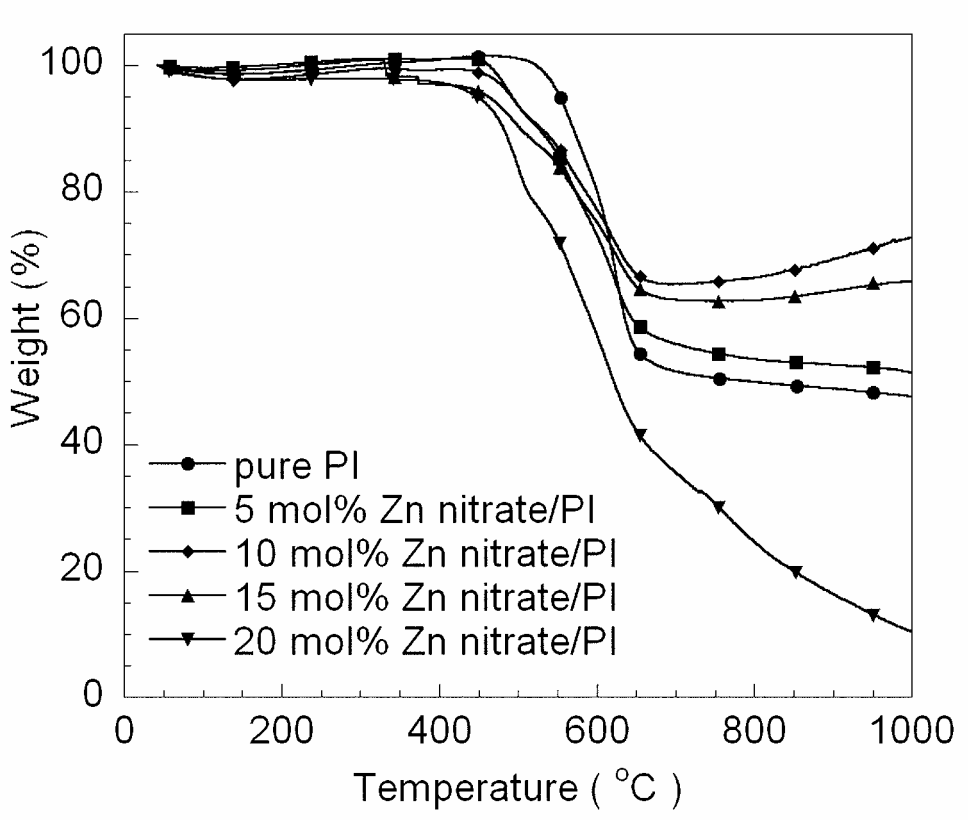

Figure 3b.

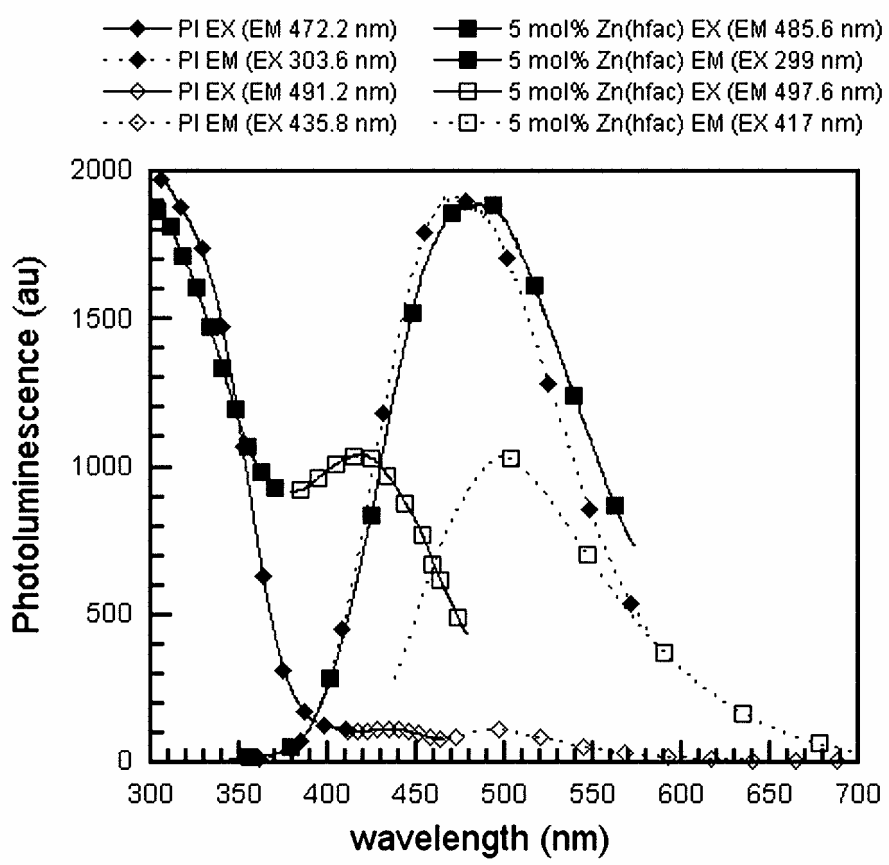

Figure 4.

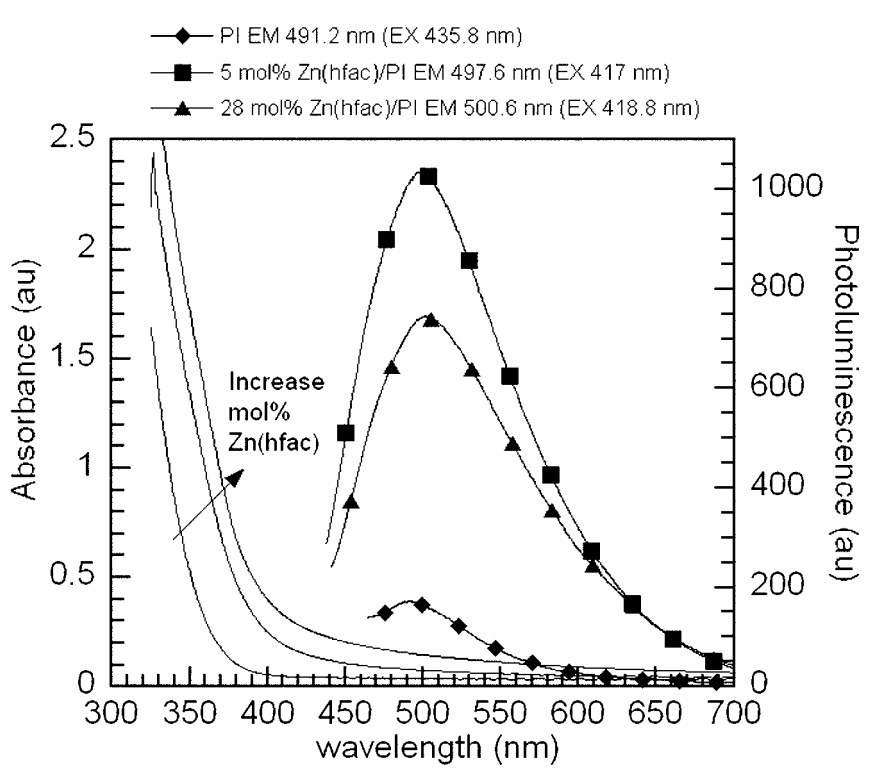

Figure 5a.

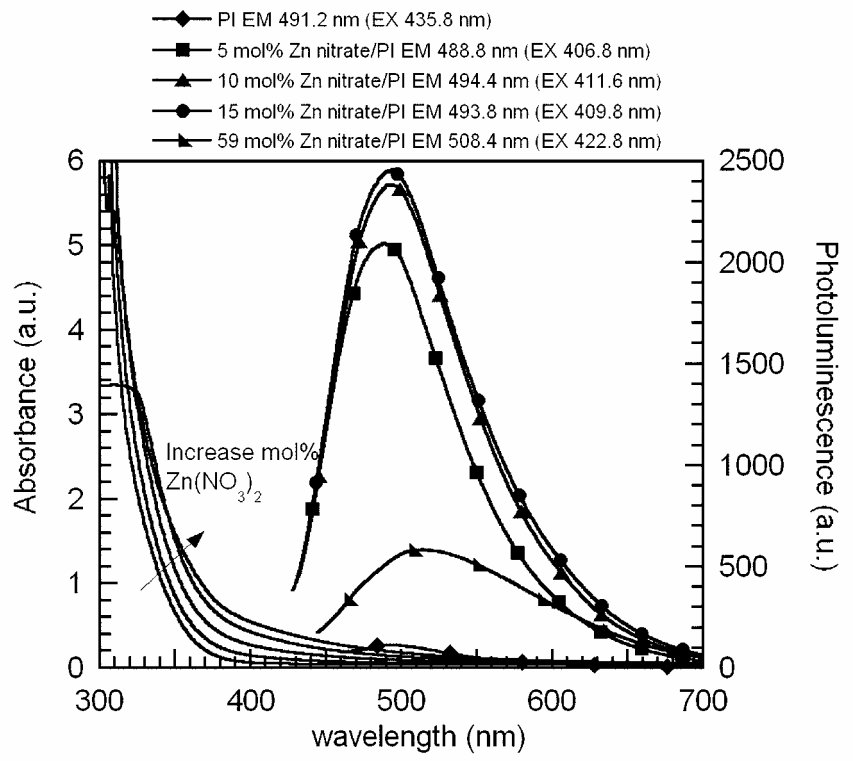

Figure 5b.

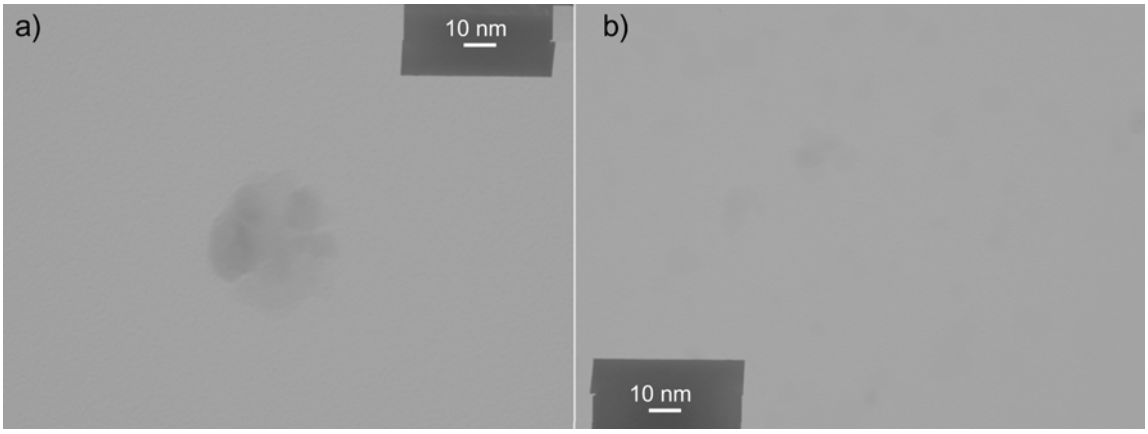

Figure 6.

ส่วนที่ 2

Effect of the origin of ZnO Nanoparticles Dispersed in Polyimide Films on their Photoluminescence and Thermal Stability

Anongnat Somwangthanaroj[*a], Chuthatai Phanthawonge[a], Shinji Ando[b] and Wiwut Tanthapanichakoon[c]

[a] Department of Chemical Engineering, Faculty of Engineering, Chulalongkorn University, Bangkok 10330, Thailand

[b] Department of Chemistry and Materials Science, Tokyo Institute of Technology, Tokyo 152-8552, Japan

[c] National Nanotechnology Center, National Science and Technology and Development Agency, Pathumtani 12120, Thailand

Abstract: Polyimide (PI) films containing dispersed ZnO nanoparticles were prepared from both zinc nitrate hexahydrate (designated as $Zn(NO_3)_2$/PI) and ZnO nanoparticles, 2-nm average primary size (ZnO/PI). This work shows how the origin of ZnO affects both the photoluminescence and thermal decomposition of the film. The presence of ZnO derived from $Zn(NO_3)_2 \cdot 6H_2O$ was confirmed by x-ray diffraction technique. The fluorescent intensities from $Zn(NO_3)_2$/PI and ZnO/PI were much higher than that from pure PI films. When the ZnO concentration exceeded a certain saturation level, the emission intensity decreased due to the undesirable aggregation of ZnO. At the same concentration, ZnO/PI exhibited higher emission intensity than $Zn(NO_3)_2$/PI. All samples prepared under nitrogen emitted higher intensity than their counterparts prepared under argon. The ZnO/PI film was thermally more stable than the $Zn(NO_3)_2$/PI one. From TEM images of 117.6 mol-% ZnO/PI films, the ZnO aggregates, whose average size was 17-90 nm, were well distributed throughout the film but poorly dispersed in nanometer range.

Keywords: fluorescence; polyimide; thermal properties; ZnO; nanoparticle

* To whom all correspondence should be addressed

Email: anongnat.s@chula.ac.th

Phone: 662-218-6864

Fax: 662-218-6877

Introduction

Polyimide was firstly reported by DuPont Co in 1960s and has been widely-known with its trade name of Kapton.[1] It shows a variety of superior properties such as thermoxidative stability, high modulus, excellent electrical properties, and chemical resistance but also showed insufficient properties important for optoelectronics and display technology such as poor radiation durability against UV light, transparency, chemical and thermal stability properties.[1] Introduction of fluorine atoms to PI improves several properties such as lower dielectric constants, higher thermal and chemical stability, radiation durability against UV light, good transparency in the visible light and NIR regions, lower refractive indices, and lower glass transition temperature of polyimides.[1] As reported by numerous researches, fluorinated PIs have been typically prepared from 4,4'-(hexafluoroisopropyllidene) diphthalic anhydride (6FDA).[2-4] These 6FDA PIs show good transparency and lower dielectric constants than those prepared from other nonfluorinated dianhydrides.[1] The fluorinated PIs, which are suitable for optical light-emitting applications, exhibit high radiation durability in the UV (λ = 200~380 nm) region, high transparency in the visible (λ=380~740 nm) and near infrared (NIR) regions (λ=740~2500 nm).

Nanocrystals of semiconducting materials have been extensively studied in the past decade for use in light emitting diodes[5] and photovoltaic solar cells[6]. An *n*-type semiconductor with a band gap of 3.4 eV and an exciton binding energy of 60 meV, zinc oxide (ZnO) is a versatile material with many applications including antireflection coating, transparent electrodes in solar cells, gas sensors, varistors, light emitting diodes and surface acoustic wave devices. At room temperature, ZnO emits ultraviolet (UV) luminescence,[7] and violet electroluminescence and blue light-emitting LED were successfully produced[8]. Therefore, much attention is now focused on the light emission properties of ZnO.

Combining ZnO nanoparticles with a polymer should enhance its optical properties such as fluorescence and radiation durability. ZnO/polymer composites have been produced with different polymer matrices, such as poly(vinylpyrrolidone)[9] and poly(hydroxyethyl methacrylate).[10] Therefore we are interested in the uniform dispersion of ZnO in PI films because of the expected superior optical characteristics such as high fluorescence, high transparency, and high radiation durability, which are suitable for applications in optoelectronics, light emitting diodes, photonics and flat-panel display

industries. This work shows how the origin of ZnO affects both the photoluminescence and thermal decomposition of the film.

Experimental Part

Materials

As shown in Figure 1, a fluorinated polyimide, 6FDA/TFDB, which exhibits good optical properties and high transparency, was synthesized from 4,4'-(hexafluoroisopropyllidene) diphthalic anhydride (6FDA) and 2,2'-bis(trifluoromethyl)-4,4'-hexafluoropropane diaminobiphenyl (TFDB). Monomers were purified by sublimation process before use. In this process, the dianhydride and diamine reacted in a dipolar aprotic solvent *N,N*-dimethylacetamide (DMAc) obtained from Aldrich Chemical Co. Zinc nitrate hexahydrate ($Zn(NO_3)_2 \cdot 6H_2O$) (99.9% purity) was also obtained from Aldrich Chemical Co. Zinc oxide nanoparticles with average primary diameters of about 2 nm were obtained from Meliorum Technologies, USA, and used as received.

Preparation of poly(amic acid) solution

As shown in Figure 1, 6FDA/TFDB-PI was prepared by the reaction between 6FDA and TFDB, which have six fluorine atoms in both monomers. More specifically, 6FDA was completely dissolved in *N,N*-dimethylacetamide (DMAc) solvent to give a clear, colorless solution. Then an equimolar amount of TFDB was slowly added to the solution with stirring to obtain a 15 wt.-% poly(amic acid) (PAA) solution. The solution was gently stirred at room temperature for 24 h. Poly(amic acid), which contains carboxamide and carboxyl group was obtained from the reaction between dianhydride from 6FDA with diamine from TFDB as shown in Figure 1.

Preparation of the ZnO/PI films

Either $Zn(NO_3)_2 \cdot 6H_2O$ or ZnO nanopowder with an average primary diameter of about 2 nm was added into the above PAA solution at the desired molar concentration of ZnO. All the synthesizing and mixing procedures were performed in argon atmosphere. Then the PAA solution was spin coated onto a glass substrate at 1000 to 1500 rpm for 15 sec to give a thin film. The film was dried at 70^{o}C for 1 h in either nitrogen or argon atmosphere and thermally imidized at curing temperature in the range of 300 to 350^{o}C for 1 h in either nitrogen or argon atmosphere, and then cooled down to room temperature. Note that there were two ways of preparing PI films embedded with ZnO nanoparticles. First, ZnO

nanoparticles were added directly to the PAA solution. Then the PAA was imidized, and the resulting nanocomposite film was designated as ZnO/PI. In the second method $Zn(NO_3)_2 \cdot 6H_2O$ was added to the PAA solution and subsequently converted to ZnO at elevated temperatures with thermal imidization of PAA. The resulting nanocomposite film was designated as $Zn(NO_3)_2$/PI. Note that the concentration of ZnO in PI films was expressed as a percentage by mole of the ZnO comparing to the repeating unit of PI.

Measurements

The luminescent property of the films was characterized by a Luminescence Spectrometer (Perkin Elmer LS 50) at room temperature using a xenon lamp as the light source. The wavelengths for excitation were in the range of 250-450 nm, and the fluorescent emission was detected in the range of 350-600 nm. The optical absorption property was characterized by a spectrophotometer (Hewlett Packard 8452A diode array) at room temperature. The wide-angle x-ray diffraction measurements (XRD) were carried out at ambient temperature using a Siemens D500 diffractometer with CuK_α radiation and Ni filter in the 2-theta range of 20-70° with a resolution of 0.02 degree·min^{-1}. The glass transition temperature was examined using a differential scanning calorimeter (DSC, diamond DSC Perkin Elmer) between 50°C and 460°C at a heating rate of 20°C·min^{-1} under nitrogen atmosphere. Thermogravimetric analysis (TGA, TA Instruments SDT Q-600) was used to determine the degradation temperature at heating rate 20 °C·min^{-1} from 35 to 1000°C under nitrogen atmosphere. The transmission electron microscopy (TEM) image was taken with an electron microscope (JEOL, JEM-2100). The PI films were embedded in epoxy resin and sectioned into a thickness of 20 nm with an ultra microtome (ultrotome V).

Results and Discussion

The XRD patterns of the PI films containing ZnO nanoparticles are shown in Figure 2. The characteristic XRD peaks, which correspond to the diffraction patterns of ZnO, indicated that ZnO crystallites are presented in the film.[11] The XRD pattern of 35.1 mol-% ZnO/PI agrees well with the wurtzite ZnO hexagonal phase which is consistent with the standard values for bulk ZnO. In addition, the positions of the first three XRD peaks of both 3.3 mol-% ZnO/PI and 666.6 mol-% $Zn(NO_3)_2$/PI are clearly observed, thereby confirming the existence of the wurtzite ZnO hexagonal phase.

Though the 35.1 mol-% ZnO/PI showed the distinct peaks indicating the presence of ZnO crystal in PI films, the XRD peaks of 3.3 mol-% ZnO/PI showed smaller and broader peaks because of its lower concentration. Interestingly, the 35.1 mol-% ZnO/PI film exhibited sharper peaks than the 666.6 mol-% $Zn(NO_3)_2$/PI film. This could be attributed to an imperfect crystal structure and smaller crystallite sizes of ZnO in the film. Average size of ZnO nanoparticles (*D*) can be estimated using the Scherrer's formula as

$$D = \frac{0.9\lambda}{\beta \cos\theta} \quad (1)$$

where λ is the wavelength of the x-ray (1.5418 °A), β is the line width at half height of the maximum peak and θ is Bragg angle of the diffraction peaks. The estimated *D* values are 13.5 and 5 nm for the 35.1mol% ZnO/PI and the 666.6 mol% $Zn(NO_3)_2$/PI, respectively.

Though the 666.6 mol-% $Zn(NO_3)_2$/PI film showed broad peaks with low intensity, it was confirmed that $Zn(NO_3)_2$ dissolved in PAA solution was successfully converted to ZnO nanoparticles by thermal decomposition. However, the 117.6 mol-% $Zn(NO_3)_2$/PI film did not show any XRD peaks, which may be due to the small crystallite size, imperfect crystal structure and too little amount of ZnO below the detection limit of the diffractometer. This result is consistent with those of Sawada and Ando's[12] and Chiang and Whang's[13].

Figure 3 shows the DSC thermograph and the estimated glass transition temperatures (T_g) for the pure PI and ZnO/PI. The T_g of 0.6 and 3.3 mol-% ZnO/PI films remained essentially the same as that of pure PI, which was 336°C, whereas the T_g of 35.1, 74.1 and 117.6 mol-% ZnO/PI slightly increased to 337.3, 338.9 and 339.4°C, respectively. This result is consistent with Hsu et al's[10] and Chae and Kim's[14]. Adding a solid filler into a polymer would reduce the mobility of the polymer chains, thereby resulting in an incremental increase in the T_g value.[15] There are two major causes to the reduction in the mobility of polymer chains in composites i.e., tethering and chain confinement [14,15]. The chain tethering is caused by the attractive forces between the filler surfaces and polymer chains. On the other hand, the chain confinement occurs when the mobility of polymer chains is significantly obstructed by the fillers. The T_g values of 35.1 mol-% and higher concentration ZnO/PI slightly increased due to the chain confinement because there was little attractive force between the surface of ZnO and polymer chains.[14] By the way, T_g was not observed in the DSC thermographs of Zn nitrate/PI (data not shown). It could be ascribed to the formation of ZnO[12, 13] during the combined decomposition and imidization

of $Zn(NO_3)_2$/PI films. The brittleness of the film may be due to the chain scission caused by generated nitric acid or ions. In addition, the formation of ZnO may affect the mobility of polymer chain, which is reflected to the obscured glass transition in $Zn(NO_3)_2$/PI film.

The presence of ZnO nanoparticles in PI films also affected their degradation temperature (T_d), which is defined as the temperature of the samples at 5 wt-% loss. It was found that the T_d of $Zn(NO_3)_2$/PI are lower than those of ZnO/PI. Figure 4 showed typical thermogravimetric profiles of $Zn(NO_3)_2$/PI films. As shown in Table 1, the addition of only 5 mol% of $Zn(NO_3)_2$ into PI decreased the T_d by 17^{o}C. However, adding more amounts of $Zn(NO_3)_2$/PI from 5 to 117.6 mol-% dramatically decrease the T_d by 17^{o}C to 204 ^{o}C. Figure 5 shows typical thermogravimetric profiles of ZnO/PI films. The T_d of these nanocomposites clearly decrease to a certain extent when adding ZnO nanoparticles directly into the films, as shown in table 1. Addition of 0.6 to 117.6 mol-% of ZnO into PI films decreases the T_d by 20^{o}- 50^{o}C. Interestingly, the ZnO/PI and $Zn(NO_3)_2$/PI films prepared at the same 35.1 mol-% concentration show different thermogravimetric profiles. The T_d of ZnO/PI decrease only by 35^{o}C compared to 132^{o}C in the case of $Zn(NO_3)_2$/PI. Obviously the ZnO/PI film has better thermal stability than the $Zn(NO_3)_2$/PI film. The difference between the T_d of ZnO/PI and that of $Zn(NO_3)_2$/PI film was a consequence of the origin of ZnO nanoparticles. Since metallic salts added into PI films induced acidic hydrolysis (chain scission) and oxidative degradation of polyimide,[12,13] the T_d of $Zn(NO_3)_2$/PI film decreased dramatically. This result was consistent with Hsu et al's[10] and Chiang and Whang's.[13]

The optical absorbance and fluorescence spectra observed for the PI films containing 35.1 mol-% ZnO at different curing temperatures are shown in Figure 6. The characteristic peaks attributable to the exciton absorption of ZnO are observed at 305 nm for all the ZnO/PI films with different curing temperatures. The absorption spectra of all films are shown in the range of 305 – 410 nm, and the absorption was quenched above 410 nm. The emission peak of all films was located at 461 nm for both 300 and 325^{o}C curing temperatures and was slightly shifted to 469 nm for the film cured at 350^{o}C. The intensity of emission slightly increased as the curing temperature increased. Though the data are not shown here, the effect of the curing temperature at a different fixed ZnO concentration exhibited a similar trend as the one just mentioned. Since the effect of curing temperature on the fluorescent intensity is slight, the curing temperature of 300^{o}C was chosen to explore the effect on fluorescence.

Figure 7 shows the effects of curing atmosphere, nitrogen or argon, on the absorbance and fluorescence at room temperature of 35.1 mol-% ZnO/PI films. The films were imidized at 300^{o}C under either nitrogen or argon atmosphere. The exciton absorption peaks of the films cured under nitrogen and argon atmosphere are observed at 302 and 307 nm, respectively. The film prepared under nitrogen shows emission and excitation peaks at 461 and 331 nm, respectively. Similarly the film prepared under argon showed peaks at 457 and 332 nm, respectively. The emission peak of the former is slightly red shifted and exhibited 2.4 times higher intensity than the latter which is consistent with Roy et al [16]. ZnO synthesized under nitrogen emitted higher intensity of green light than that prepared under argon which could be due to different intrinsic defects in ZnO such as oxygen vacancy and interstitial zinc. The effect of the curing atmosphere at other ZnO concentrations exhibited similar trends (the spectra are not shown here).

The effects of ZnO concentration on the fluorescence and absorbance were presented in Figures 8 - 11. All the films were imidized at 300^{o}C under nitrogen. As expected, the existence of ZnO in PI films enhanced the fluorescence emission. Figure 8 and 9 show the effect of ZnO/PI concentration on the optical absorption and emission intensity, respectively. As the concentration of ZnO nanoparticles increases from 0.6-117.6 mol-%, Figure 8 shows that the exciton absorption peak is blue shifted from 318 to 295 nm and the absorbance decreased. This phenomenon is caused by the broadened distribution of aggregates of ZnO nanoparticles in the PI film, which was confirmed by TEM image (Figure 13). All samples exhibited absorption spectra in the range of 300 – 370 nm. Above 370 nm, the absorbance of pure PI, 0.6 and 3.3 mol-% ZnO/PI films was quenched in the visible region. However, some incremental absorbance intensity in the visible region (above 370 nm) was detected in high-concentration ZnO/PI films (> 35.1 mol-% ZnO) due to the presence of submicron-size ZnO particles, which was confirmed by TEM micrograph (Figure 13). The high-concentration ZnO/PI films are less transparent than the corresponding $Zn(NO_3)_2$/PI films because submicron-sized ZnO cause significant light scattering in the visible region.

Figure 9 shows that, as the concentration of ZnO nanoparticles increased to 3.3 mol-%, the fluorescent intensity increased and was slightly blue shifted from 474 to 458 nm compared to that of pure PI, although the wavelength of the excitation peak of all films was approximately the same (except the case of 117.6 mol-% ZnO). As the concentration of ZnO nanoparticles increased to 35.1 mol-% and above, the fluorescent intensity is,

however, not shifted further compared to that of 3.3 mol-% ZnO/PI. More specifically, at 0.6 and 35.1 mol-% of ZnO nanoparticles, the fluorescent intensity at visible wavelength was enhanced by 2.2 and 7.8 times compared to that of pure PI. However, adding more amounts of ZnO nanoparticles at 74.1 and 117.6 mol-% to the films, the light emission intensity was dramatically decreased due to the self-absorption of ZnO. Fluorescence was generally inversely proportional to the concentration owing to the concentration quenching,[17] which can be classified into two categories: self-quenching and self-absorption. Self-quenching is a collision phenomenon between molecules in the ground state and those in excited state conditions, which leads to the energy transfer without fluorescence. On the other hand, self-absorption is a phenomenon in which the wavelength of fluorescence overlaps that of the absorption by the sample. In other words, the fluorescence was absorbed by the other molecules. This is consistent with the appearance of an increase in the absorption in the visible region (above 370 nm). Moreover, the emission in the visible region at all concentrations of ZnO nanoparticles except 0.6 mol-% in PI films showed two main peaks at 460 and 485 nm, similar to the result by Roy et al [16]. The peak appearing at 485 nm could be originated from oxygen vacancy defect in ZnO.

Similarly, the effects of ZnO concentration from thermal decomposition of $Zn(NO_3)_2$ in PI films on the absorbance and fluorescence of Zn nitrate/PI films were shown in Figures 10 and 11, respectively. In Figure10, $Zn(NO_3)_2$/PI films of all concentrations exhibit broad absorption in the range of 300 – 370 nm with peaks around 318 nm. The absorption above 370 nm gradually increase as the concentration of $Zn(NO_3)_2$ increase due to the increase in particle size of ZnO as confirmed by XRD. However, the exciton absorption peak at all Zn nitrate concentrations was not shifted compared to that of the ZnO/PI films.

Figure 11 showed the effect of ZnO concentration in $Zn(NO_3)_2$/PI films on the fluorescent intensity and wavelength. Adding only 5 mol-% of $Zn(NO_3)_2$ to the PI film shows the highest intensity in the visible region compared to all other concentrations. In fact, the fluorescent intensity of 5 mol-% Zn nitrate/PI was 1.9 times that of the pure PI. On the other hand, the intensities of 10 and 15 mol-% Zn $(NO_3)_2$/PI are lower than that of 5 mol-% $Zn(NO_3)_2$/PI, whereas the fluorescent intensity of 35.1, 74.1 and 117.6 mol-% $Zn(NO_3)_2$/PI films became even lower than that of pure PI as the concentration increases owing to the aggregation of ZnO nanoparticles. Moreover, the emission peak of these $Zn(NO_3)_2$/PI films was red shifted when compared to that of the pure PI films, which may

also be attributed to the aggregation of ZnO nanoparticles. This result is consistent with the appearance of the increasing absorption above 370 nm. In contrast, the light emission of ZnO/PI was slightly blue shifted because of no change in the size of ZnO nanoparticles in the PI films, which was confirmed by TEM image (Figure 13).

By the way, the visible light emission of 5, 10 and 15 mol-% $Zn(NO_3)_2$/PI showed two main peaks at 486 and 502 nm, similar to the results reported by Roy et al.[16] In addition, all samples emitted green color. The visible light emission was assumed to be caused by different intrinsic defects in ZnO such as oxygen vacancy and interstitial zinc (450-600 nm).[18-20]

Figure 12 showed the effect of the origin of ZnO on the absorbance and fluorescence of PI films at the same ZnO concentration of 35.1 mol-%. The films were imidized at 300^{o}C under nitrogen. The exciton absorption peaks of $Zn(NO_3)_2$/PI and ZnO/PI are observed at 313 and 301 nm, respectively. Both PI films show absorption bands in the range of 300-400 nm. However, an increase in absorbance (above 400 nm) was observed for ZnO/PI compared to that of $Zn(NO_3)_2$/PI. Furthermore, the fluorescence of ZnO/PI shows an emission peak at 461 nm, which is significantly blue shifted from the 491 nm of $Zn(NO_3)_2$/PI, and also exhibits a much higher intensity. The excitation and emission peaks of ZnO/PI are enhanced by 8.7 times than those of $Zn(NO_3)_2$/PI, which is attributed to an imperfect crystal structure and smaller crystallite sizes of ZnO nanoparticles in $Zn(NO_3)_2$/PI films (confirmed with XRD data). In addition, the ZnO generated from the thermal decomposition of $Zn(NO_3)_2$ in PI films results in more self-quenching than ZnO nanoparticles dispersed in ZnO/PI films.

The transmission electron microscopy (TEM) images of 117.6 mol-% ZnO/PI films are shown in Figure 13(a) and 13(b). Obviously the ZnO nanoparticles are well distributed throughout the film but poorly dispersed in PI films as can be seen in figure 13(a). The diameter of ZnO primary particle obtained from the vendor is around 2 nm. The aggregates of ZnO nanoparticles with an average diameter of 17 – 90 nm are observed in Figure 13(b) and approximately agglomeration of ZnO nanoparticles with average size of 114-150 nm is also observed. However, small ZnO nanoparticles generated from the thermal decomposition of $Zn(NO_3)_2$ are not observed in this study mainly due to the limitation of TEM resolution capacity (data not shown).

Conclusion

The thermal conversion of zinc nitrate hexahydrate ($Zn(NO_3)_2 \cdot 6H_2O$) to zinc oxide (ZnO) nanoparticles was confirmed by XRD technique. The glass transition temperature (T_g) of ZnO nano-particle-dispersed polyimide films (ZnO/PI) slightly increase when the concentration of ZnO nanoparticles is higher than 35.1 mol-%, which is due to the confinement of polymer chain mobility by ZnO . However, no T_g of $Zn(NO_3)_2$/PI were observed in the film. The 5 wt-% degradation temperatures (T_d) of all nanocomposite films are lower than that of pure PI, though the ZnO/PI films exhibits higher thermal stability than $Zn(NO_3)_2$/PI films.

The 35.1 mol-% ZnO/PI exhibits fluorescence with the highest intensity, which is 7.8 times as high as that of pure PI. In fact, the fluorescent intensities of all ZnO/PI films are higher than that of pure PI. An addition of only 5 mol-% $Zn(NO_3)_2$ enhances the fluorescence by 1.9 times compared with that of pure PI. Moreover, the light emission of $Zn(NO_3)_2$/PI films shows a red shift compared to that of pure PI. This may be attributed to the aggregation of ZnO nanoparticles. As for the effect of the curing atmosphere on fluorescence, the films prepared under nitrogen emit higher fluorescent intensity than those prepared under argon. However, the curing temperature gives slightly effect on the fluorescent intensity. The TEM images show ZnO nanoparticles embedded in PI films in which the aggregates with an average diameter of 17 – 90 nm are observed. In addition, ZnO nanoparticles agglomerate with average size of 114-150 nm. In other words, ZnO nanoparticles are well distributed but poorly dispersed in the PI films. It is expected that the optical properties of the ZnO-containing PI films would be further enhanced if the ZnO nanoparticles could be uniformly distributed and dispersed as primary particles in the films.

Acknowledgments: The authors acknowledge Thailand Research Fund (TRF) and Thailand-Japan Technology Transfer Project (TJTTP) for financial support. We thank Dr. Toemsak Srikhirin, Department of Physics, Faculty of Science, Mahidol University for use of luminescence spectrometer and spectrophotometer for this study.

References

1. Ghosh, M. K.; Mittal, K. L. Polyimides foundamentals and applications; Marcel Dekker: New York, 1996.
2. Chiron, D.; Trigaud, T.; Moliton, J. P. Synthetic Metals 2001, 124, 33.
3. Cornic, C.; Lucas, B.; Moliton, A.; Colombeau, B.; Mercier, R. Synthetic Metals 2002, 127, 299.

4. Kim, J. H.; Koros, W. J.; Paul, D. R. Polymer 2006, 47, 3104.
5. Kim, H.; Horwitz, J. S.; Kim, W. H.; Ma¨kinen, A. J.; Kafafi, Z. H.; Chrisey, D. B. Thin Solid Films 2002, 420-421, 539.
6. Cembrero, J.; Elmanouni, A.; Hartiti, B.; Mollar, M.; Mari, B. Thin Solid Films 2004, 451-452, 198.
7. Hirai, T.; Harada, Y.; Hashimoto, S.; Itoh, T.; Ohno, N. Journal of Luminescence 2004, 112, 196.
8. Tsukazaki, A.; Ohtomo, A.; Onuma, T.; Ohtani, M.; Makino, T.; Sumiya, M.; Ohtani, K.; Chichibu, S. F.; Fuke, S.; Segawa, Y.; Ohno, H.; Koinuma, H.; Kawasaki, M. Nature Materials 2005, 4, 42.
9. Guo, L.; Yang, S.; Yang, C.; Yu, P.; Wang, J.; Ge, W.; Wong, G. K. L. Chemistry of Materials 2003, 12, 2268
10. Hsu, S. C.; Whang, W. T.; Hung, C. H.; Chiang, P. C.; Hsiao, Y. N. Macromol Chem Phys 2005, 206, 291.
11. Andelman, T.; Gong, Y.; Polking, M.; Yin, M.; Kuskovsky, I.; Neumark, G.; O'Brien, S. The journal of physical chemistry B 2005, 109, 14314.
12. Sawada, T.; Ando, S. Chemistry of Materials 1998, 10, 3368
13. Chiang, P. C.; Whang, W. T. Polymer 2003, 44, 2249.
14. Chae, D. W.; Kim, B. C. Polymers for Advanced Technologies 2005, 16, 846.
15. Savin, D. A.; Pyun, J.; Patterson, G. D.; Kowalewski, T.; Matyjaszewski, K. J Polym Sci Pol Phys 2002, 40, 2667.
16. Roy, V. A. L.; Djurisic, A. B.; Chan, W. K.; Gao, J.; Lui, H. F.; Surya, C. Applied Physics Letters 2003, 83, 141.
17. Lawan, S. Fluorometric analysis; Faculty of Pharmaceutical sciences Sillapakron University: Nakonpatom, 2544.
18. Lin, B.; Fu, Z.; Jia, Y. Applied Physics Letters 2001, 79, 943.
19. Lin, Y.; Xie, J.; Wang, H.; Li, Y.; Chavez, C.; Lee, S. Y.; Foltyn, S. R.; Crooker, S. A.; Burrell, A. K.; McCleskey, T. M.; Jia, Q. X. Thin Solid Films 2005, 492, 101.
20. Masuda, Y.; Kinoshita, N.; Sato, F.; Koumoto, K. Crystal Growth and Design 2006, 6, 75.

Caption of table

Table 1. The degradation temperature of pure PI, ZnO/PI and Zn nitrate/PI.

Caption of figures

Figure 1. Chemical structures of monomers and preparation process of poly(amic acid) and polyimide

Figure 2. XRD patterns of pure PI, PI with ZnO nanoparticles from thermal decomposition of $Zn(NO_3)_2$ hexahydrate and ZnO nanoparticles directly added into PI.

Figure 3. DSC heating thermograms of PI containing directly added ZnO nanoparticles.

Figure 4. Thermogravimetric profiles of PI containing ZnO nanoparticles from thermal decomposition of $Zn(NO_3)_2$ hexahydrate.

Figure 5. Thermogravimetric profiles of PI containing directly added ZnO nanoparticles.

Figure 6. Effect of curing temperature on fluorescence of 35.1 mol-% ZnO/PI cured under nitrogen atmosphere.

Figure 7. Effect of curing atmosphere on fluorescence of 35.1 mol-% ZnO/PI cured at $300^{\circ}C$.

Figure 8. Effect of ZnO concentration on absorbance of ZnO/PI cured under nitrogen atmosphere at $300^{\circ}C$.

Figure 9. Effect of ZnO concentration on fluorescence of ZnO/PI cured under nitrogen atmosphere at $300^{\circ}C$.

Figure 10. Effect of ZnO concentration on absorbance of Zn nitrate/PI cured under nitrogen atmosphere at $300^{\circ}C$.

Figure 11. Effect of ZnO concentration on fluorescence of Zn nitrate/PI cured under nitrogen atmosphere at $300^{\circ}C$.

Figure 12. Effect of the origin of ZnO at concentration of 35.1 mol-% on fluorescence cured under nitrogen atmosphere at $300^{\circ}C$.

Figure 13. TEM images of polyimide containing 117.6 mol-% ZnO nanoparticles (a) low magnification image (x 12,000) (b) high magnification image (x 120,000)

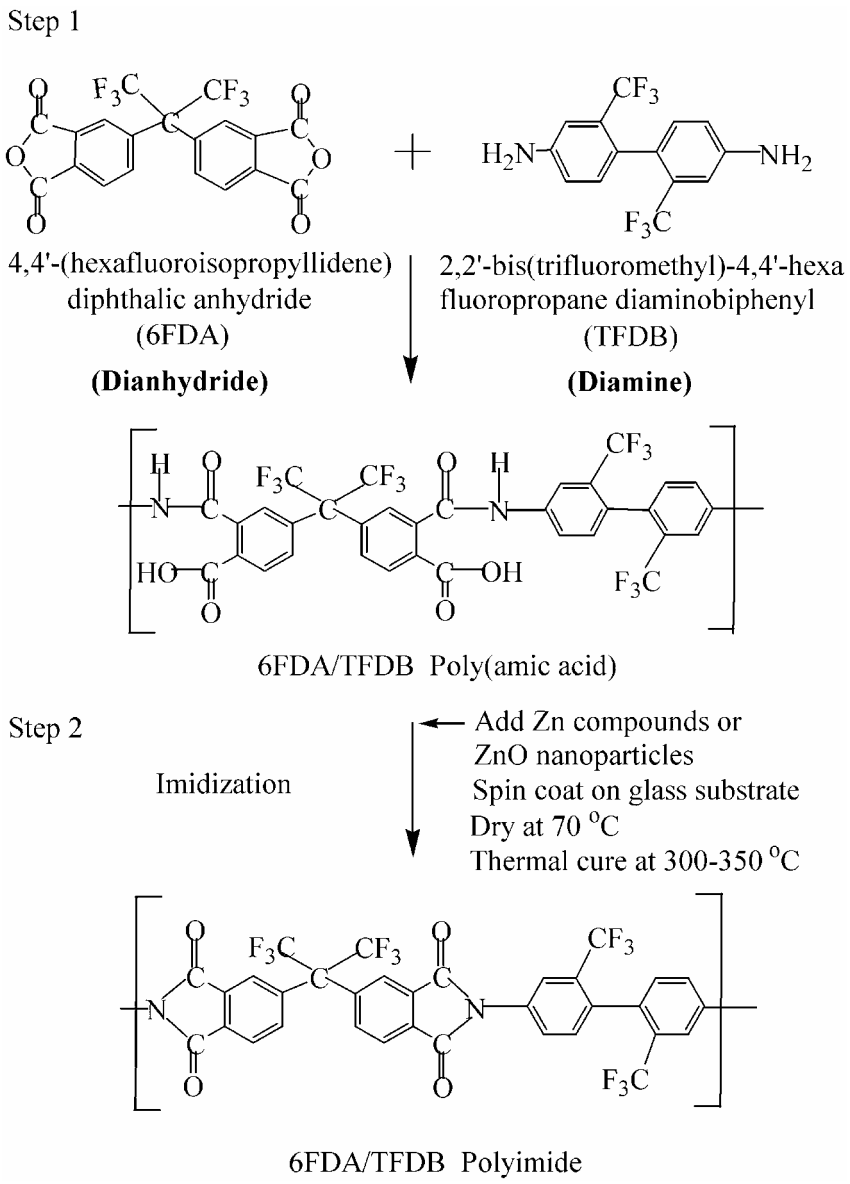
Step 1
4,4'-(hexafluoroisopropyllidene) diphthalic anhydride (6FDA)
(Dianhydride)
2,2'-bis(trifluoromethyl)-4,4'-hexa fluoropropane diaminobiphenyl (TFDB)
(Diamine)
6FDA/TFDB Poly(amic acid)
Step 2
Imidization
Add Zn compounds or ZnO nanoparticles
Spin coat on glass substrate
Dry at 70 °C
Thermal cure at 300-350 °C
6FDA/TFDB Polyimide

Figure 1.

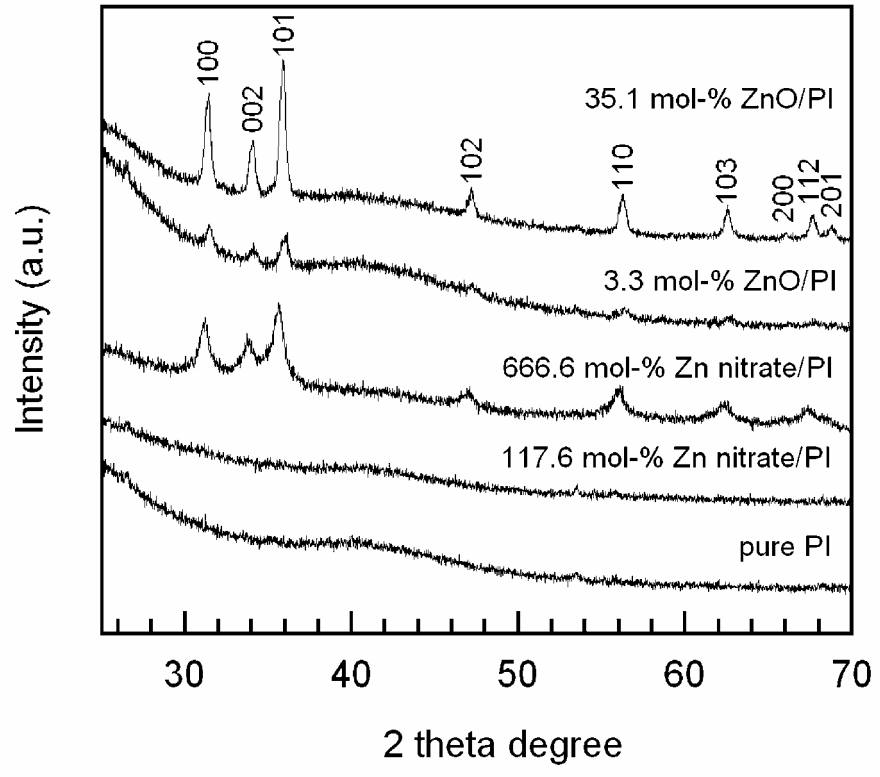

Figure 2.

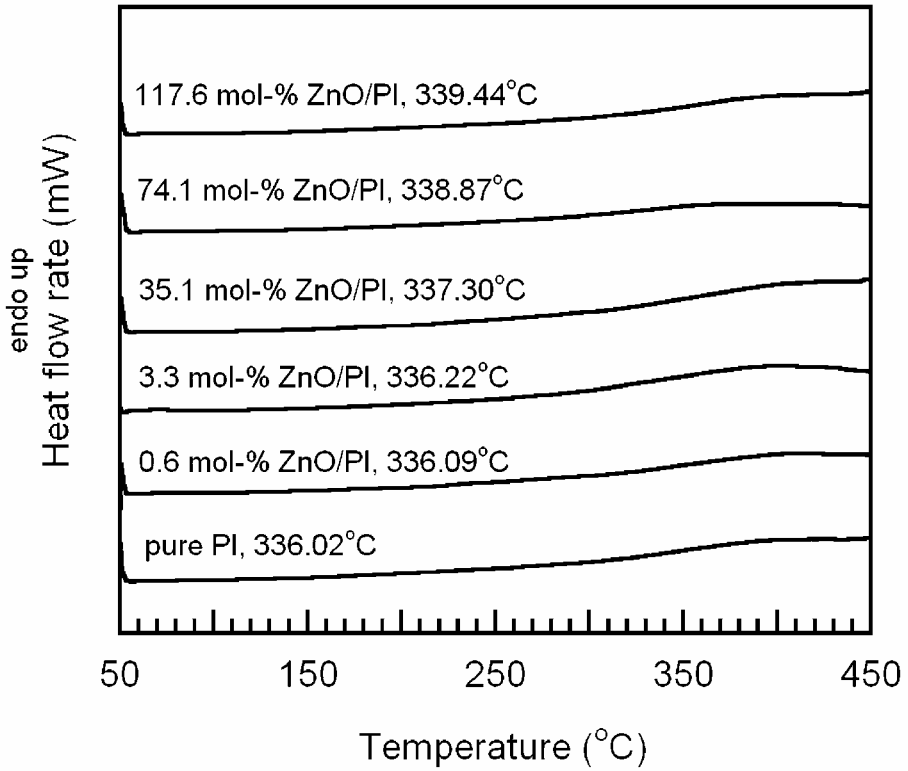

Figure 3.

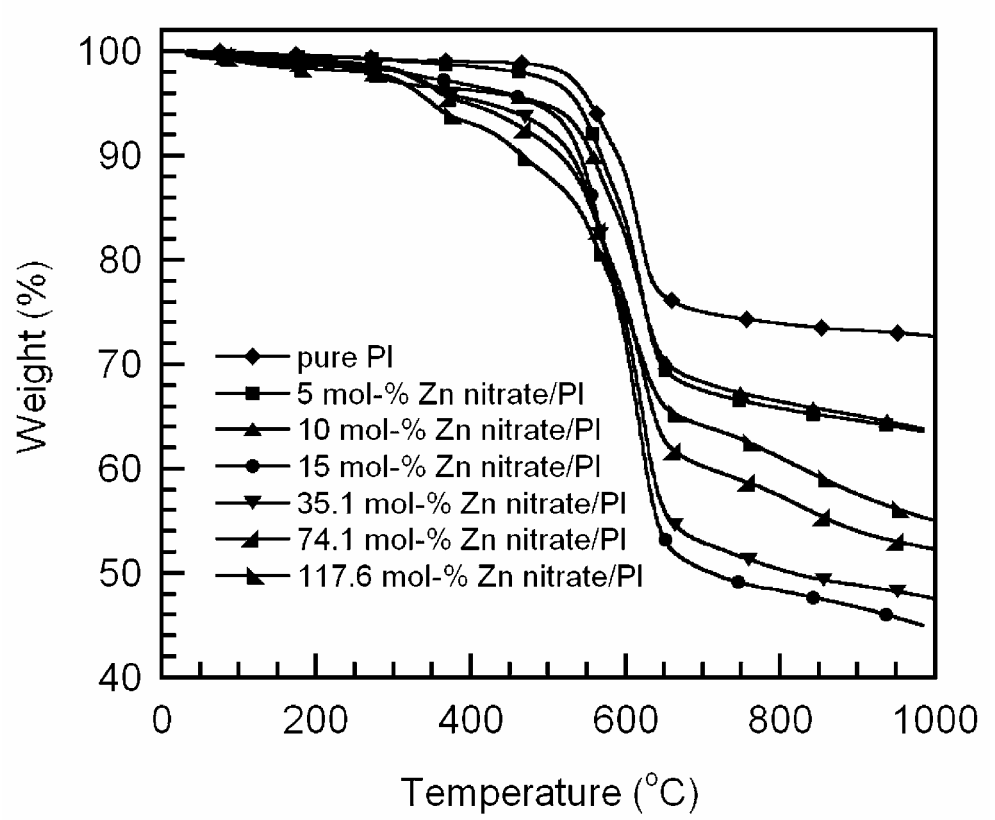

Figure 4.

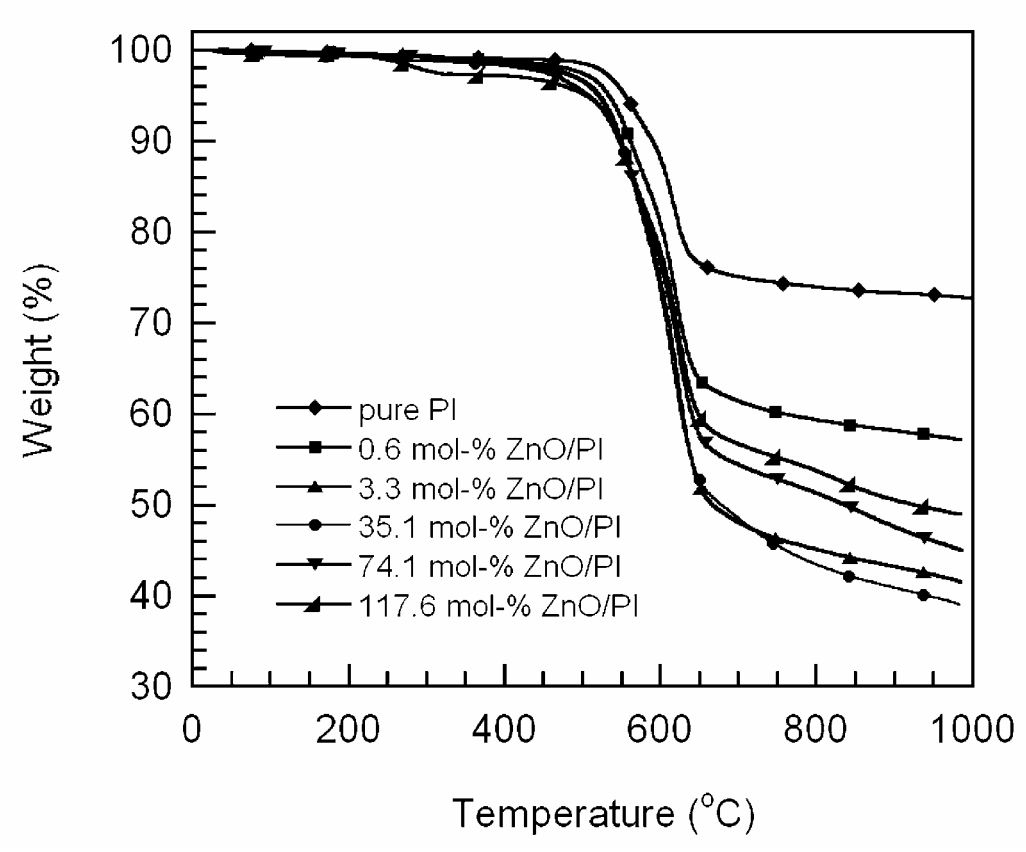

Figure 5.

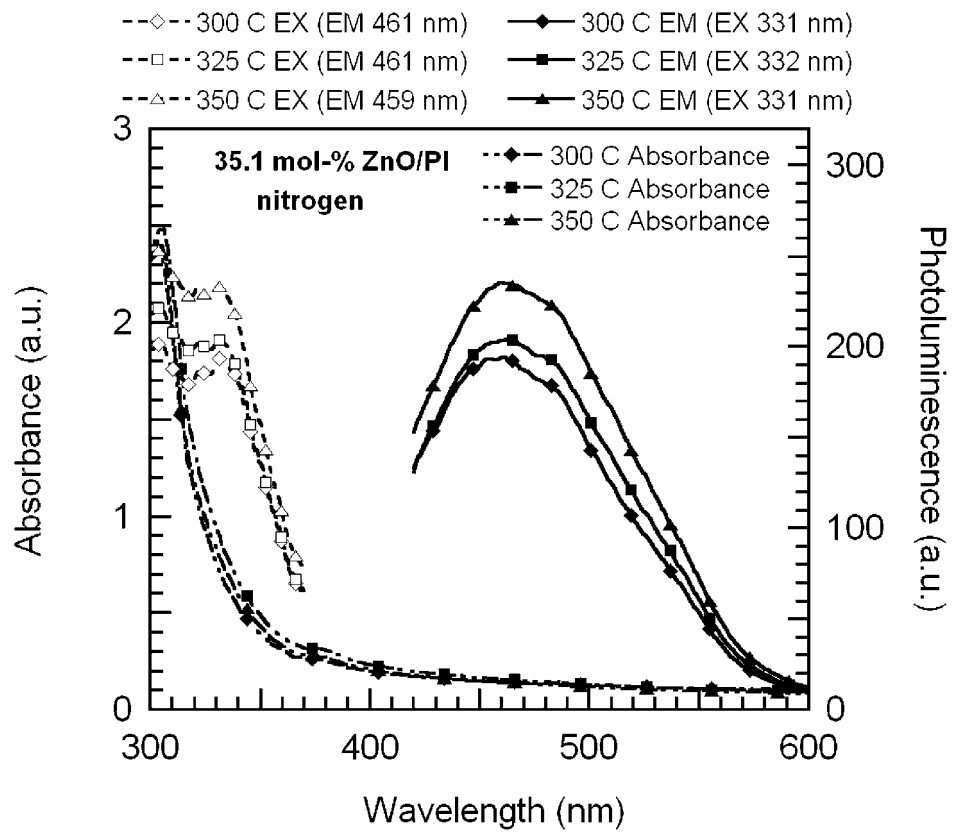

Figure 6.

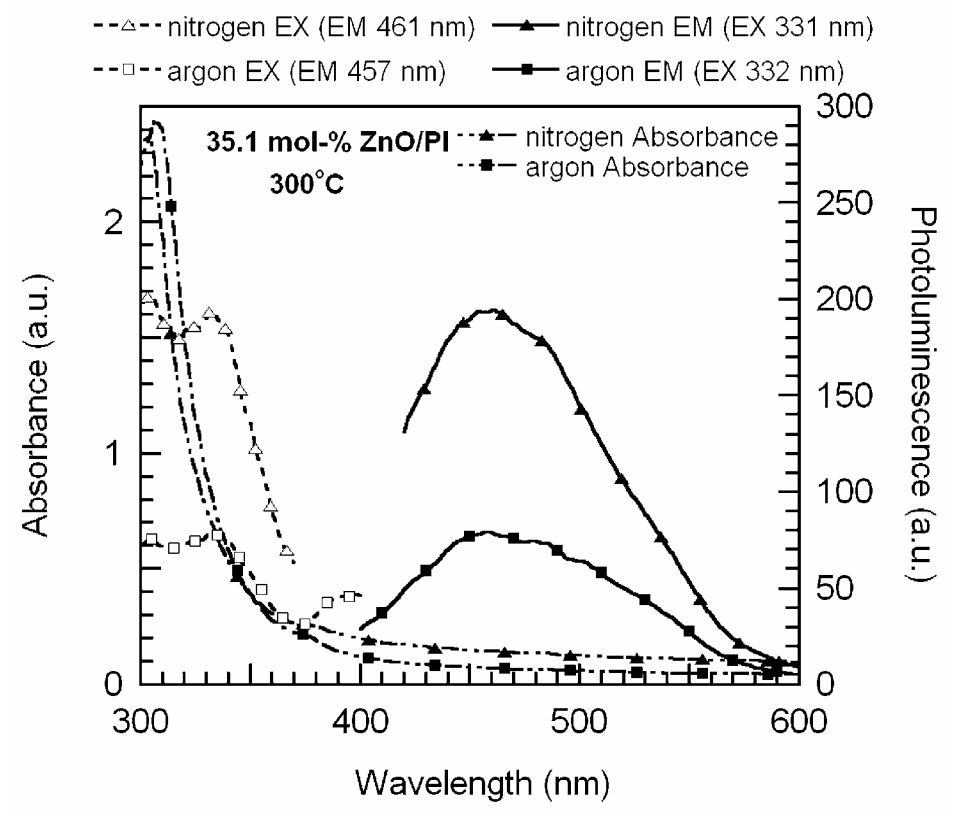

Figure 7.

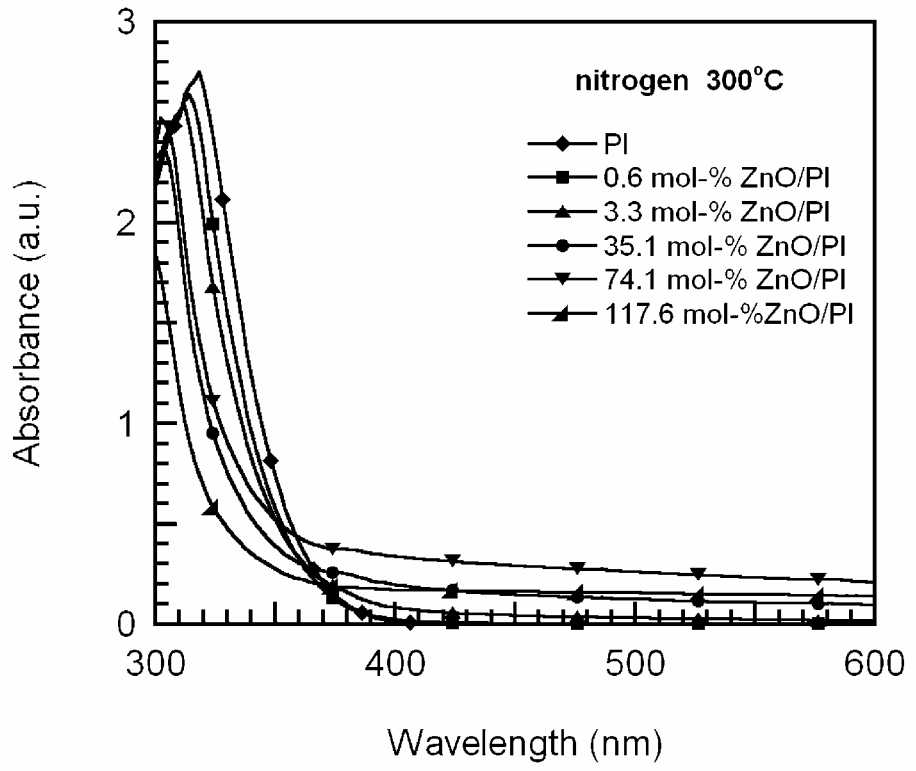

Figure 8.

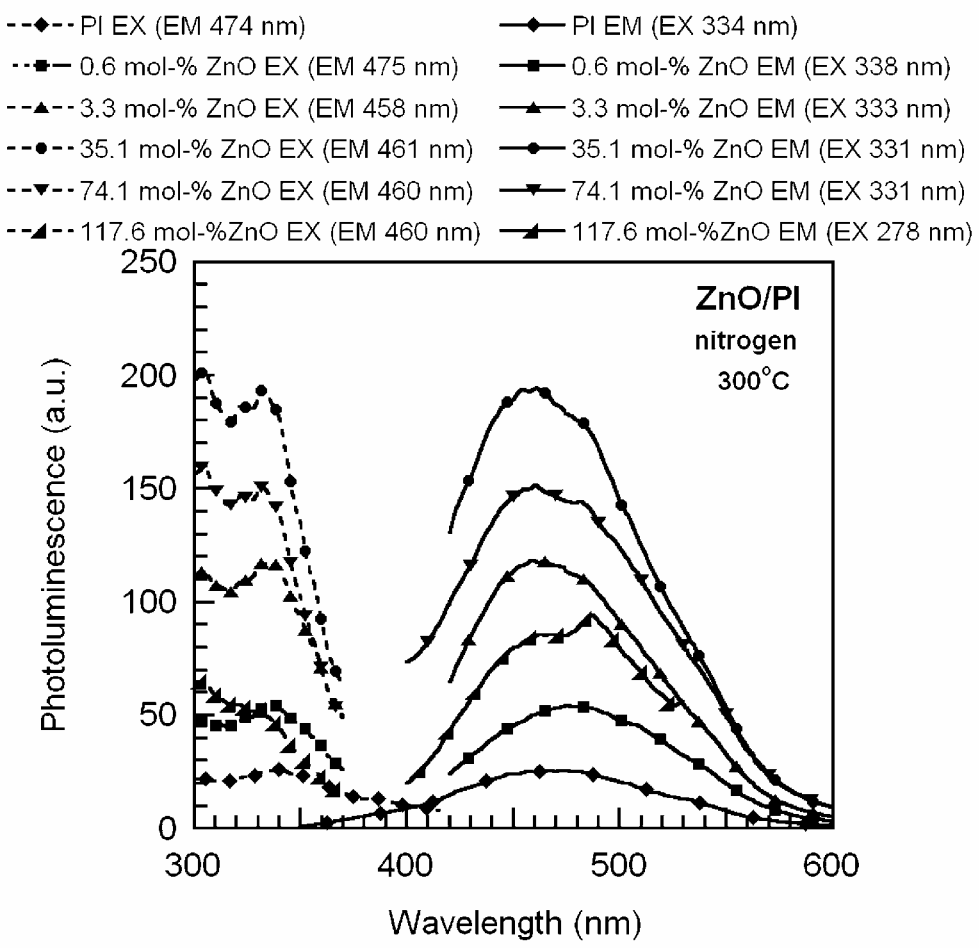

Figure 9.

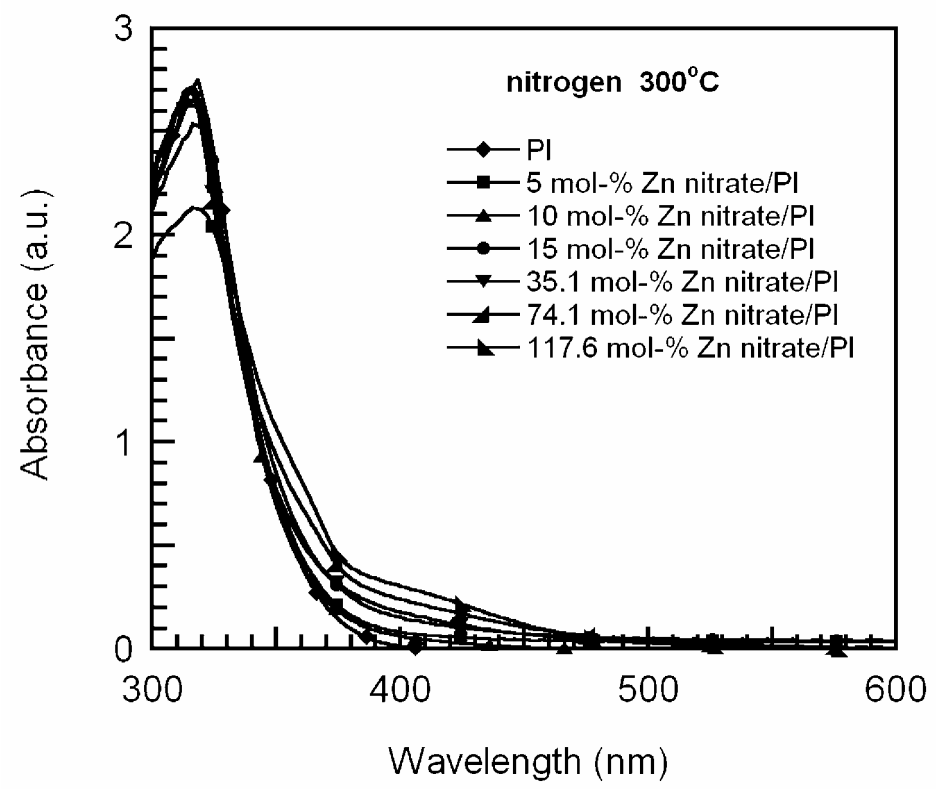

Figure 10.

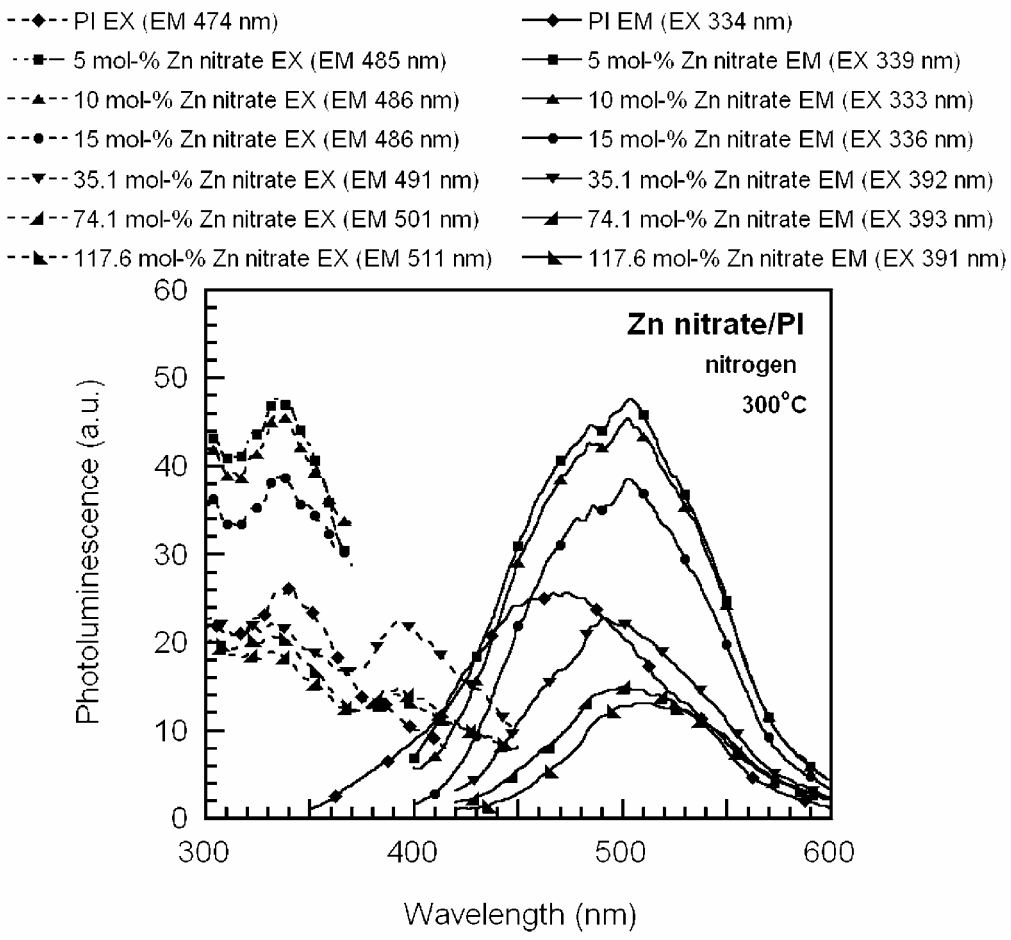

Figure 11.

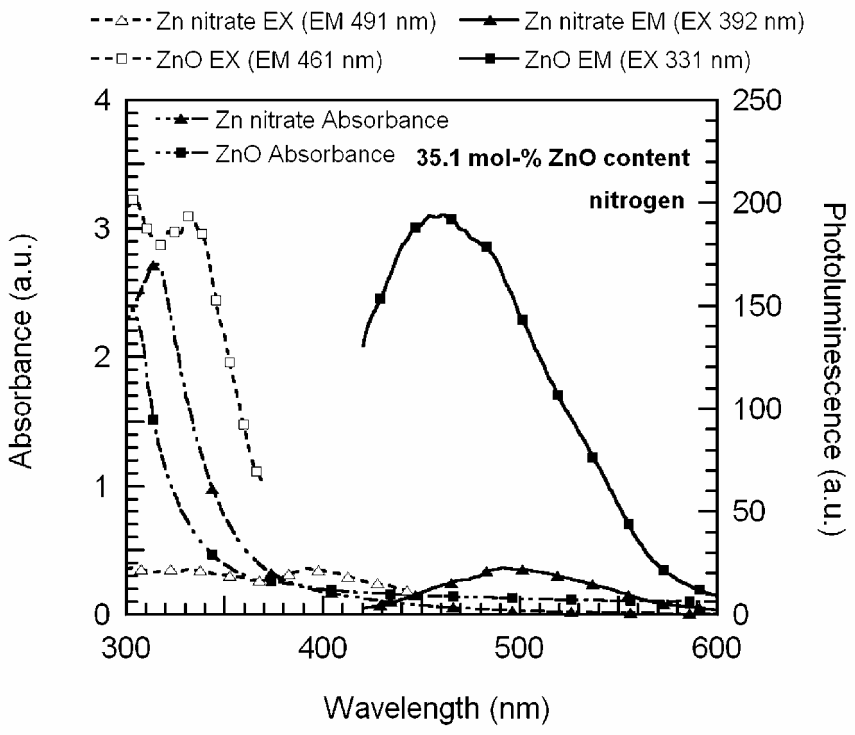
Zn nitrate EX (EM 491 nm)
Zn nitrate EM (EX 392 nm)
ZnO EX (EM 461 nm)
ZnO EM (EX 331 nm)
Zn nitrate Absorbance
ZnO Absorbance
35.1 mol-% ZnO content
nitrogen
Absorbance (a.u.)
Photoluminescence (a.u.)
Wavelength (nm)
0
1
2
3
4
0
50
100
150
200
250
300
400
500
600

Figure 12.

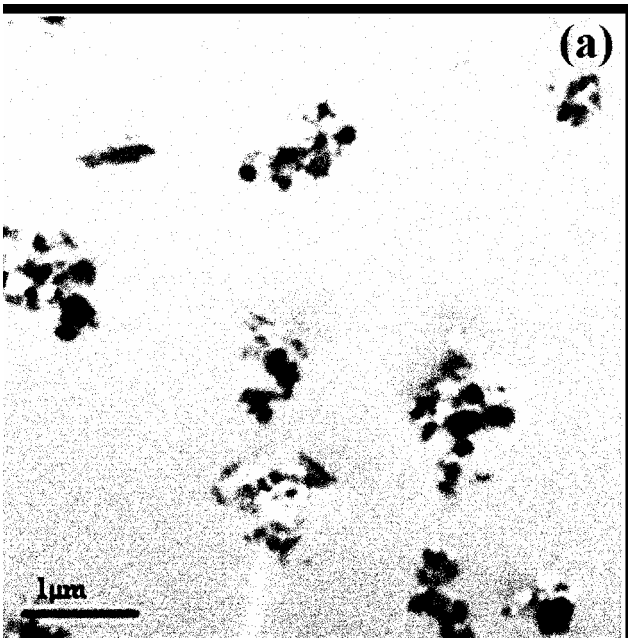

Figure 13a.

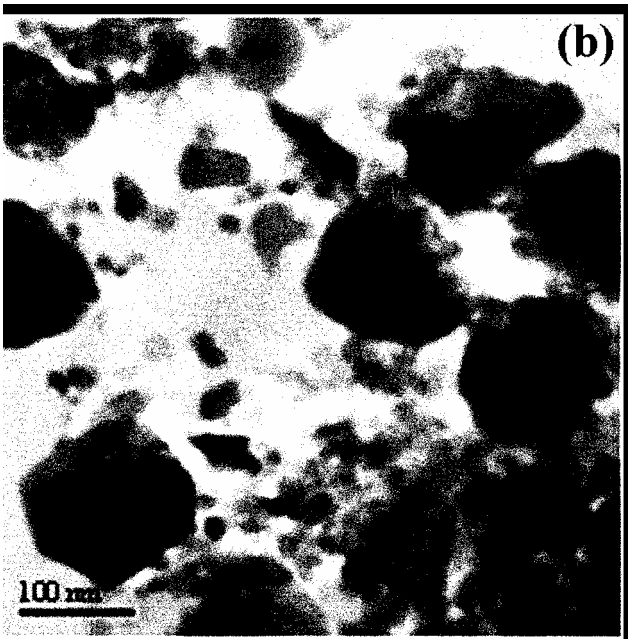

Figure 13b.

Output จากโครงการวิจัยที่ได้รับทุนจาก สกว.

1. ผลงานตีพิมพ์ในวารสารวิชาการนานาชาติ

1.1 Anongnat Somwangthanaroj, Chuthatai Phanthawonge, Shinji Ando and Wiwut Tanthapanichakoon, "*Effect of the origin of ZnO Nanoparticles Dispersed in Polyimide Films on their Photoluminescence and Thermal Stability*," Journal of Applied Polymer Science, 2008, in press

1.2 Anongnat Somwangthanaroj, Kanokwan Suwanchatchai, Shinji Ando and Wiwut Tanthapanichakoon, *"Effect of zinc precursor on thermal and light emission properties of ZnO nanoparticles embedded in polyimide films via thermal decomposition process,*" submitted

2. การนำผลงานวิจัยไปใช้ประโยชน์

- เชิงวิชาการ (มีการพัฒนาการเรียนการสอน/สร้างนักวิจัยใหม่)
  - งานวิจัยนี้เป็นการพัฒนาวัสดุชนิดใหม่ทำให้สามารถนำไปเป็นตัวอย่างในการสอนวิชาพอลิเมอร์ได้ นอกจากนี้ยังเป็นการฝึกนิสิตระดับปริญญาโท ในการทำการค้นคว้าวิจัยภายใต้การดูแลของผู้วิจัย

3. การเสนอผลงานในที่ประชุมวิชาการ

3.1 A. Somwangthanaroj, C. Phanthawonge, S. Ando and W. Tanthapanichakoon, "*Light Emission Properties of Dispersed ZnO- nanoparticles in Polyimide Films*," presented at Regional Symposium on Chemical Engineering (RSCE) Annual Meeting, Singapore, December 3 -5, 2006

3.2 A. Somwangthanaroj, C. Phanthawonge, S. Ando and W. Tanthapanichakoon, *"In-situ Preparation by Thermal Decomposition Process and Green - light Emitting Properties of ZnO Nanoparticles Dispersed in Fluorinated Polyimide Films,*" presented at การประชุม "นักวิจัยรุ่นใหม่ พบ เมธีวิจัยอาวุโส สกว." ครั้งที่ 7, Chonburi, Thailand, October 11 – 13, 2007

3.3 A. Somwangthanaroj, C. Phanthawonge, S. Ando and W. Tanthapanichakoon, *"Photoluminescence and Thermal Stability of Zno Nanoparticles Dispersed in Polyimide Films"* presented at the 10th Pacific Polymer Conference (PPC 10), Kobe, Japan, December 4 – 7, 2007

Journal of Applied Polymer Science

Copy of e-mail Notification

YOUR PROOFS (2007-11-3481.R1) FROM Journal of Applied Polymer Science ARE AVAILABLE FOR CORRECTIONS
=====
Journal of Applied Polymer Science Published by John Wiley & Sons, Inc.

Dear Author,

YOUR PAGE PROOFS ARE AVAILABLE IN PDF FORMAT; please refer to this URL address http://kwglobal.co.in/jw/retrieval.aspx

Login: your e-mail address
Password: ----

The site contains 1 file. You will need to have Adobe Acrobat Reader software to read these files. This is free software and is available for user downloading at http://www.adobe.com/products/acrobat/readstep.html. If you have the Notes annotation tool (not contained within Acrobat reader), you can make corrections electronically and return them to Wiley as an e-mail attachment (see the Notes tool instruction sheet). Alternatively, if you would prefer to receive a paper proof by regular mail, please contact Birender/Sundeep at wileysupport@kwglobal.com or +91(44)4205-8888 (ext. 310). Be sure to include your article number.

This file contains:

Author Instructions Checklist
Adobe Acrobat Users - NOTES tool sheet
Reprint Order form
A copy of your page proofs for your article

After printing the PDF file, please read the page proofs carefully and:

1) indicate changes or corrections in the margin of the page proofs;
2) answer all queries (footnotes A,B,C, etc.) on the last page of the PDF proof;
3) proofread any tables and equations carefully;
4) check that any Greek, especially "mu", has translated correctly.

Special Notes:

Please return hard copy corrections and reprint order form to Wiley via express/overnight service or fax as soon as possible (to the APP Journal Team; see address and numbers below). If you fax your corrections, please include a cover page detailing the corrections as changes may be distorted during transmission. If you have access to Adobe Acrobat 6.0 or 7.0, annotated PDF files may be returned via e-mail.

Your article will be published online via our EarlyView service after correction receipt. Your prompt attention to and return of page proofs is crucial to faster publication of your work. Thank you for your cooperation.

Journal of Applied Polymer Science

Copy of e-mail Notification

Return to:

APP Journal Team
John Wiley & Sons, Inc.
111 River Street
Hoboken, NJ 07030
U.S.A.
(See fax number and e-mail address below.)

If you experience technical problems, please contact Birender/Sundeep at wileysupport@kwglobal.com or +91(44)4205-8888 (ext. 310).

If you have any questions regarding your article, please contact me. PLEASE ALWAYS INCLUDE YOUR ARTICLE NO. (200 -11-3481. 1) WITH ALL CORRESPONDENCE.

This e-proof is to be used only for the purpose of returning corrections to the publisher.

Sincerely,

APP Journal Team
John Wiley & Sons, Inc.
E-mail: APPjournal@wiley.com
Tel: 201-748-8659
Fax: 201-748-6052

WILEY
Publishers Since 1807

111 River Street, Hoboken, NJ 07030

*****IMMEDIATE RESPONSE REQUIRED*****
Please follow these instructions to avoid delay of publication.

☐ **READ PROOFS CAREFULLY**

- This will be your only chance to review these proofs.
- Please note that the volume and page numbers shown on the proofs are for position only.

☐ **ANSWER ALL QUERIES ON PROOFS** (Queries for you to answer are attached as the last page of your proof.)

- Mark all corrections directly on the proofs. Note that excessive author alterations may ultimately result in delay of publication and extra costs may be charged to you.

☐ **CHECK FIGURES AND TABLES CAREFULLY** (Color figures will be sent under separate cover.)

- Check size, numbering, and orientation of figures.
- All images in the PDF are downsampled (reduced to lower resolution and file size) to facilitate Internet delivery. These images will appear at higher resolution and sharpness in the printed article.
- Review figure legends to ensure that they are complete.
- Check all tables. Review layout, title, and footnotes.

☐ **COMPLETE REPRINT ORDER FORM**

- Fill out the attached reprint order form. It is important to return the form even if you are not ordering reprints. You may, if you wish, pay for the reprints with a credit card. Reprints will be mailed only after your article appears in print. This is the most opportune time to order reprints. If you wait until after your article comes off press, the reprints will be considerably more expensive.

RETURN ☐**PROOFS**
☐**REPRINT ORDER FORM**
☐**CTA (If you have not already signed one)**

RETURN WITHIN 48 HOURS OF RECEIPT VIA FAX TO 201-748-6052

QUESTIONS?

APP Journal Team
Phone: 201-748-8659
E-mail: APPjournal@wiley.com
Refer to journal acronym and article production number

Softproofing for advanced Adobe Acrobat Users - NOTES tool

NOTE: ACROBAT READER FROM THE INTERNET DOES NOT CONTAIN THE NOTES TOOL USED IN THIS PROCEDURE.

Acrobat annotation tools can be very useful for indicating changes to the PDF proof of your article. By using Acrobat annotation tools, a full digital pathway can be maintained for your page proofs.

The NOTES annotation tool can be used with either Adobe Acrobat 6.0 or Adobe Acrobat 7.0. Other annotation tools are also available in Acrobat 6.0, but this instruction sheet will concentrate on how to use the NOTES tool. Acrobat Reader, the free Internet download software from Adobe, DOES NOT contain the NOTES tool. In order to softproof using the NOTES tool you must have the full software suite Adobe Acrobat Exchange 6.0 or Adobe Acrobat 7.0 installed on your computer.

Steps for Softproofing using Adobe Acrobat NOTES tool:

1. Open the PDF page proof of your article using either Adobe Acrobat Exchange 6.0 or Adobe Acrobat 7.0. Proof your article on-screen or print a copy for markup of changes.

2. Go to Edit/Preferences/Commenting (in Acrobat 6.0) or Edit/Preferences/Commenting (in Acrobat 7.0) check “Always use login name for author name” option. Also, set the font size at 9 or 10 point.

3. When you have decided on the corrections to your article, select the NOTES tool from the Acrobat toolbox (Acrobat 6.0) and click to display note text to be changed, or Comments/Add Note (in Acrobat 7.0).

4. Enter your corrections into the NOTES text box window. Be sure to clearly indicate where the correction is to be placed and what text it will effect. If necessary to avoid confusion, you can use your TEXT SELECTION tool to copy the text to be corrected and paste it into the NOTES text box window. At this point, you can type the corrections directly into the NOTES text box window. **DO NOT correct the text by typing directly on the PDF page.**

5. Go through your entire article using the NOTES tool as described in Step 4.

6. When you have completed the corrections to your article, go to Document/Export Comments (in Acrobat 6.0) or Comments/Export Comments (in Acrobat 7.0). Save your NOTES file to a place on your harddrive where you can easily locate it. **Name your NOTES file with the article number assigned to your article in the original softproofing e-mail message.**

7. **When closing your article PDF be sure NOT to save changes to original file.**

8. To make changes to a NOTES file you have exported, simply re-open the original PDF proof file, go to Document/Import Comments and import the NOTES file you saved. Make changes and reexport NOTES file keeping the same file name.

9. When complete, attach your NOTES file to a reply e-mail message. Be sure to include your name, the date, and the title of the journal your article will be printed in.

John Wiley & Sons, Inc.

Publishers Since 1807

REPRINT BILLING DEPARTMENT • 111 RIVER STREET • HOBOKEN, NJ 07030
PHONE: (201) 748-8789; FAX: (201) 748-6326
E-MAIL: reprints @ wiley.com

PREPUBLICATION REPRINT ORDER FORM

Please complete this form even if you are not ordering reprints. This form **MUST** be returned with your corrected proofs and original manuscript. Your reprints will be shipped approximately 4 weeks after publication. Reprints ordered after printing are substantially more expensive.

JOURNAL: ***JOURNAL OF APPLIED POLYMER SCIENCE*** VOLUME_____ ISSUE_____

TITLE OF MANUSCRIPT_____

MS. NO._____ NO. OF PAGES_____ AUTHOR(S)_____

REPRINTS 8 1/4 X 11

No. of Pages	100 Reprints	200 Reprints	300 Reprints	400 Reprints	500 Reprints
	$	$	$	$	$
1-4	336	501	694	890	1,052
5-8	469	703	987	1,251	1,477
9-12	594	923	1,234	1,565	1,850
13-16	714	1,156	1,527	1,901	2,273
17-20	794	1,340	1,775	2,212	2,648
21-24	911	1,529	2,031	2,536	3,037
25-28	1,004	1,707	2,267	2,828	3,388
29-32	1,108	1,894	2,515	3,135	3,755
33-36	1,219	2,092	2,773	3,456	4,143
37-40	1,329	2,290	3,033	3,776	4,528

****** REPRINTS ARE ONLY AVAILABLE IN LOTS OF 100. IF YOU WISH TO ORDER MORE THAN 500 REPRINTS, PLEASE CONTACT OUR REPRINTS DEPARTMENT AT (201)748-8789 FOR A PRICE QUOTE.

COVERS

100 Covers - $90 • 200 Covers - $145 • 300 Covers - $200
400 Covers - $255 • 500 Covers - $325 • Additional 100s - $65

❑ Please send me _____ reprints of the above article at..... $_____
❑ Please send me _____ Generic covers of the above journal at..... $_____
Please add appropriate State and Local Tax {Tax Exempt No._____} $_____
Please add 5% Postage and Handling..... $_____
TOTAL AMOUNT OF ORDER** ..... $_____

***International orders must be paid in U.S. currency and drawn on a U.S. bank*

Please check one: ❑ Check enclosed ❑ Bill me ❑ Credit Card
If credit card order, charge to: ❑ American Express ❑ Visa ❑ MasterCard ❑ Discover
Credit Card No._____ Signature_____ Exp. Date_____

Bill To:

Name_____
Address/Institution_____
_____
_____
_____
Purchase Order No. _____ Phone _____ Fax _____

Ship To:

Name_____
Address/Institution_____
_____
_____
_____
E-mail: _____

111 RIVER STREET, HOBOKEN, NJ 07030

Telephone Number: • Facsimile Number:

To: APP JOURNAL TEAM

Company:

Phone: 201-748-8659

Fax: 201-748-6052

From:

Date:

Pages including this cover page:

Message:

Re:

Effect of the Origin of ZnO Nanoparticles Dispersed in Polyimide Films on Their Photoluminescence and Thermal Stability

Anongnat Somwangthanaroj,[1] Chuthatai Phanthawonge,[1] Shinji Ando,[2] Wiwut Tanthapanichakoon[3]

[1]*Department of Chemical Engineering, Faculty of Engineering, Chulalongkorn University, Bangkok 10330, Thailand*
[2]*Department of Chemistry and Materials Science, Tokyo Institute of Technology, Tokyo 152-8552, Japan*
[3]*National Nanotechnology Center, National Science and Technology and Development Agency, Pathumtani 12120, Thailand*

Received 13 November 2007; accepted 26 February 2008
DOI 10.1002/app.28299
Published online in Wiley InterScience (www.interscience.wiley.com).

ABSTRACT: Polyimide (PI) films containing dispersed ZnO nanoparticles were prepared from both zinc nitrate hexahydrate (designated as $Zn(NO_3)_2$/PI) and ZnO nanoparticles, 2-nm average primary size (ZnO/PI). This work shows how the origin of ZnO affects both the photoluminescence and thermal decomposition of the film. The presence of ZnO derived from $Zn(NO_3)_2{\cdot}6H_2O$ was confirmed by X-ray diffraction technique. The fluorescent intensities from $Zn(NO_3)_2$/PI and ZnO/PI were much higher than that from pure PI films. When the ZnO concentration exceeded a certain saturation level, the emission intensity decreased due to the undesirable aggregation of ZnO. At the same concentration, ZnO/PI exhibited higher emission intensity than $Zn(NO_3)_2$/PI. All samples prepared under nitrogen emitted higher intensity than their counterparts prepared under argon. The ZnO/PI film was thermally more stable than the $Zn(NO_3)_2$/PI one. From TEM images of 117.6 mol% ZnO/PI films, the ZnO aggregates, whose average size was 17–90 nm, were well distributed throughout the film but poorly dispersed in nanometer range. J Appl Polym Sci 000: 000–000, 2008

Key words: fluorescence; polyimide; thermal properties; ZnO; nanoparticle

INTRODUCTION

Polyimide (PI) was firstly reported by DuPont Co in 1960s and has been widely-known with its trade name of Kapton.[1] It shows a variety of superior properties such as thermoxidative stability, high modulus, excellent electrical properties, and chemical resistance but also showed insufficient properties important for optoelectronics and display technology such as poor radiation durability against UV light, transparency, chemical, and thermal stability properties.[1] Introduction of fluorine atoms to PI improves several properties such as lower dielectric constants, higher thermal, and chemical stability, radiation durability against UV light, good transparency in the visible light and NIR regions, lower refractive indices, and lower glass transition temperature of polyimides.[1] As reported by numerous researches, fluorinated PIs have been typically prepared from 4,4′-(hexafluoroisopropyllidene) diphthalic anhydride (6FDA).[2–4] These 6FDA PIs show good transparency and lower dielectric constants than those prepared from other nonfluorinated dianhydrides.[1] The fluorinated PIs, which are suitable for optical light-emitting applications, exhibit high radiation durability in the UV (λ = 200–380 nm) region, high transparency in the visible (λ = 380–740 nm) and near infrared (NIR) regions (λ = 740–2500 nm).

Nanocrystals of semiconducting materials have been extensively studied in the past decade for use in light emitting diodes[5] and photovoltaic solar cells.[6] An *n*-type semiconductor with a band gap of 3.4 eV and an exciton binding energy of 60 meV, zinc oxide (ZnO) is a versatile material with many applications including antireflection coating, transparent electrodes in solar cells, gas sensors, varistors, light emitting diodes, and surface acoustic wave devices. At room temperature, ZnO emits ultraviolet (UV) luminescence,[7] and violet electroluminescence and blue light-emitting LED were successfully produced.[8] Therefore, much attention is now focused on the light emission properties of ZnO.

Combining ZnO nanoparticles with a polymer should enhance its optical properties such as fluorescence and radiation durability. ZnO/polymer

Correspondence to: A. Somwangthanaroj (anongnat.s@chula.ac.th).

Contract grant sponsors: Thailand Research Fund (TRF), Thailand-Japan Technology Transfer Project (TJTTP).

J_ID: Z8E Customer A_ID: APP28299 Date: 15-APRIL-08 Stage: I Page: 2

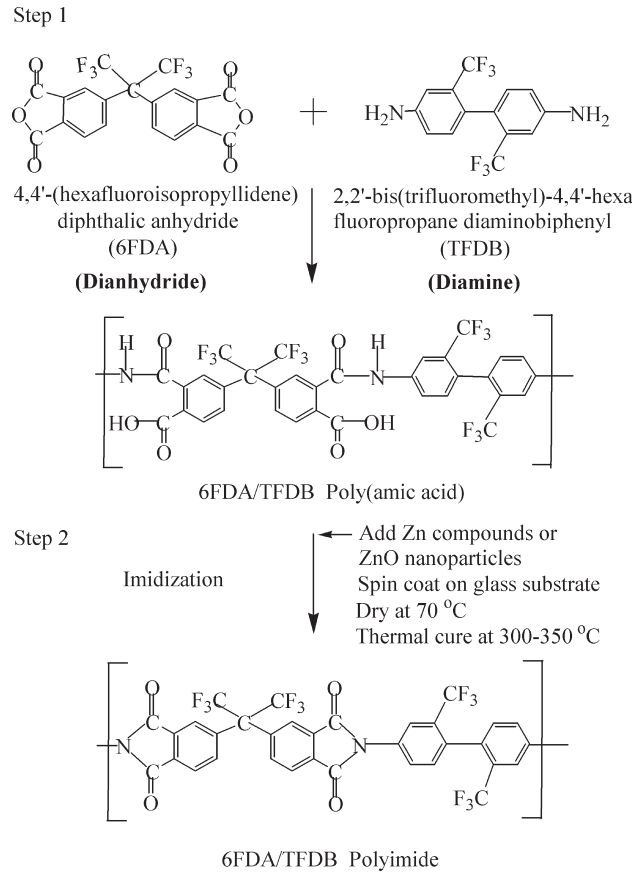

Figure 1 Chemical structures of monomers and preparation process of poly(amic acid) and polyimide.

composites have been produced with different polymer matrices, such as poly(vinyl pyrrolidone)[9] and poly (hydroxyethyl methacrylate).[10] Therefore we are interested in the uniform dispersion of ZnO in PI films because of the expected superior optical characteristics such as high fluorescence, high transparency, and high radiation durability, which are suitable for applications in optoelectronics, light emitting diodes, photonics and flat-panel display industries. This work shows how the origin of ZnO affects both the photoluminescence and thermal decomposition of the film.

EXPERIMENTAL

Materials

F1 As shown in Figure 1, a fluorinated polyimide, 6FDA/TFDB, which exhibits good optical properties and high transparency, was synthesized from 4,4′-(hexafluoroisopropyllidene) diphthalic anhydride (6FDA) and 2,2′-bis(trifluoromethyl)-4,4′-hexafluoropropane diaminobiphenyl (TFDB). Monomers were purified by sublimation process before use. In this process, the dianhydride and diamine reacted in a dipolar aprotic solvent *N,N*-dimethylacetamide (DMAc) obtained from Aldrich Chemical. Zinc nitrate hexahydrate ($Zn(NO_3)_2{\cdot}6H_2O$) (99.9% purity) was also obtained from Aldrich Chemical. Zinc oxide nanoparticles with average primary diameters of about 2 nm were obtained from Meliorum Technologies, USA, and used as received.

Preparation of poly(amic acid) solution

As shown in Figure 1, 6 FDA/TFDB-PI was prepared by the reaction between 6FDA and TFDB, which have six fluorine atoms in both monomers. More specifically, 6FDA was completely dissolved in *N,N*-dimethylacetamide (DMAc) solvent to give a clear, colorless solution. Then an equimolar amount of TFDB was slowly added to the solution with stirring to obtain a 15 wt % poly(amic acid) (PAA) solution. The solution was gently stirred at room temperature for 24 h. Poly(amic acid), which contains carboxamide and carboxyl group was obtained from the reaction between dianhydride from 6FDA with diamine from TFDB as shown in Figure 1.

Preparation of the ZnO/PI films

Either $Zn(NO_3)_2{\cdot}6H_2O$ or ZnO nanopowder with an average primary diameter of about 2 nm was added into the above PAA solution at the desired molar concentration of ZnO. All the synthesizing and mixing procedures were performed in argon atmosphere. Then the PAA solution was spin coated onto a glass substrate at 1000–1500 rpm for 15 s to give a thin film. The film was dried at 70°C for 1 h in either nitrogen or argon atmosphere and thermally imidized at curing temperature in the range of 300–350°C for 1 h in either nitrogenor argon atmosphere, and then cooled down to room temperature. Note that there were two ways of preparing PI films embedded with ZnO nanoparticles. First, ZnO nanoparticles were added directly to the PAA solution. Then the PAA was imidized, and the resulting nanocomposite film was designated as ZnO/PI. In the second method $Zn(NO_3)_2{\cdot}6H_2O$ was added to the PAA solution and subsequently converted to ZnO at elevated temperatures with thermal imidization of PAA. The resulting nanocomposite film was designated as $Zn(NO_3)_2$/PI. Note that the concentration of ZnO in PI films was expressed as a percentage by mole of the ZnO comparing to the repeating unit of PI.

Measurements

The luminescent property of the films was characterized by a Luminescence Spectrometer (Perkin–Elmer LS 50) at room temperature using a xenon lamp as the light source. The wavelengths for excitation were

ID: 40410 Date: 15/4/08 Time: 17:56 Path: J:/Production/APP#/Vol00000/080384/3B2/C2APP#080384

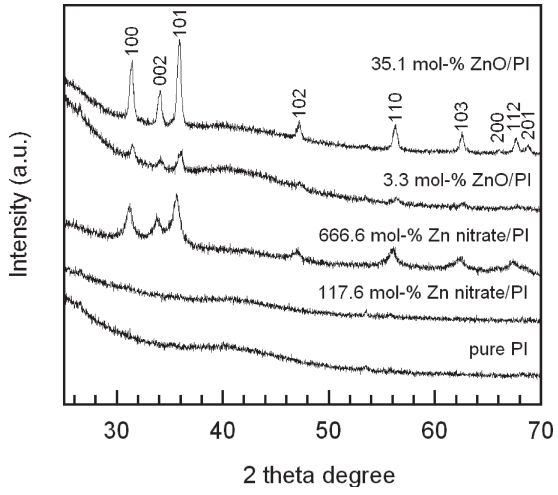

Figure 2 XRD patterns of pure PI, PI with ZnO nanoparticles from thermal decomposition of $Zn(NO_3)_2$ hexahydrate and ZnO nanoparticles directly added into PI.

in the range of 250–450 nm, and the fluorescent emission was detected in the range of 350–600 nm. The optical absorption property was characterized by a spectrophotometer (Hewlett–Packard 8452A diode array) at room temperature. The wide-angle X-ray diffraction measurements (XRD) were carried out at ambient temperature using a Siemens D500 diffractometer with Cu$K\alpha$ radiation and Ni filter in the 2θ range of 20°–70° with a resolution of 0.02° min^{-1}. The glass transition temperature was examined using a differential scanning calorimeter (DSC, diamond DSC Perkin-Elmer) between 50 and 460°C at a heating rate of 20°C min^{-1} under nitrogen atmosphere. Thermogravimetric analysis (TGA, TA Instruments SDT Q-600) was used to determine the degradation temperature at heating rate 20°C min^{-1} from 35 to 1000°C under nitrogen atmosphere. The transmission electron microscopy (TEM) image was taken with an electron microscope (JEOL, JEM-2100). The PI films were embedded in epoxy resin and sectioned into a thickness of 20 nm with an ultra microtome (ultrotome V).

RESULTS AND DISCUSSION

The XRD patterns of the PI films containing ZnO nanoparticles are shown in Figure 2. The characteristic XRD peaks, which correspond to the diffraction patterns of ZnO, indicated that ZnO crystallites are presented in the film.[11] The XRD pattern of 35.1 mol % ZnO/PI agrees well with the wurtzite ZnO hexagonal phase which is consistent with the standard values for bulk ZnO. In addition, the positions of the first three XRD peaks of both 3.3 mol % ZnO/PI and 666.6 mol % $Zn(NO_3)_2$/PI are clearly observed, thereby confirming the existence of the wurtzite ZnO hexagonal phase.

Though the 35.1 mol % ZnO/PI showed the distinct peaks indicating the presence of ZnO crystal in PI films, the XRD peaks of 3.3 mol % ZnO/PI showed smaller and broader peaks because of its lower concentration. Interestingly, the 35.1 mol % ZnO/PI film exhibited sharper peaks than the 666.6 mol % $Zn(NO_3)_2$/PI film. This could be attributed to an imperfect crystal structure and smaller crystallite sizes of ZnO in the film. Average size of ZnO nanoparticles (D) can be estimated using the Scherrer's formula as

$$D = \frac{0.9\lambda}{\beta\cos\theta} \quad (1)$$

where λ is the wavelength of the X-ray (1.5418°A), β is the line width at half height of the maximum peak and θ is Bragg angle of the diffraction peaks. The estimated D values are 13.5 and 5 nm for the 35.1 mol % ZnO/PI and the 666.6 mol % $Zn(NO_3)_2$/PI, respectively.

Though the 666.6 mol % $Zn(NO_3)_2$/PI film showed broad peaks with low intensity, it was confirmed that $Zn(NO_3)_2$ dissolved in PAA solution was successfully converted to ZnO nanoparticles by thermal decomposition. However, the 117.6 mol % $Zn(NO_3)_2$/PI film did not show any XRD peaks, which may be due to the small crystallite size, imperfect crystal structure and too little amount of ZnO below the detection limit of the diffractometer. This result is consistent with those of Sawada and Ando's[12] and Chiang and Whang's[13].

Figure 3 shows the DSC thermograph and the estimated glass transition temperatures (T_g) for the pure PI and ZnO/PI. The T_g of 0.6 and 3.3 mol % ZnO/PI films remained essentially the same as that of pure

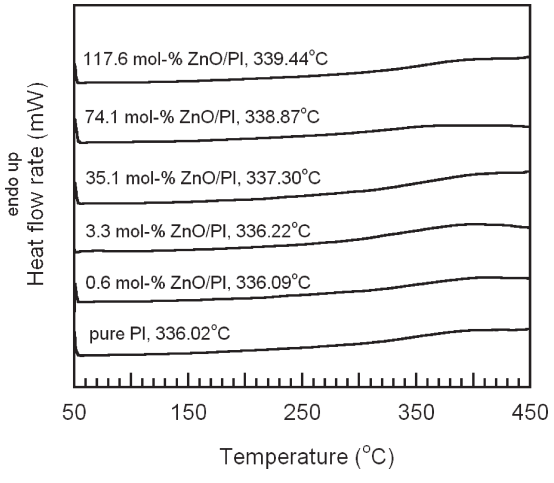

Figure 3 DSC heating thermograms of PI containing directly added ZnO nanoparticles.

J_ID: Z8E Customer A_ID: APP28299 Date: 15-APRIL-08 Stage: I Page: 4

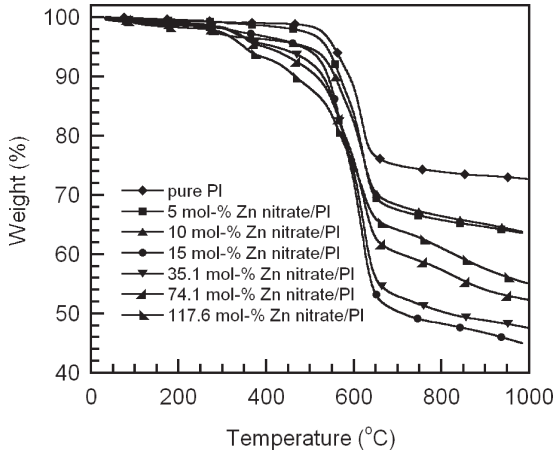

Figure 4 Thermogravimetric profiles of PI containing ZnO nanoparticles from thermal decomposition of $Zn(NO_3)_2$ hexahydrate.

PI, which was 336°C, whereas the T_g of 35.1, 74.1, and 117.6 mol % ZnO/PI slightly increased to 337.3, 338.9, and 339.4°C, respectively. This result is consistent with Hsu et al.'s [10] and Chae and Kim's[14]. Adding a solid filler into a polymer would reduce the mobility of the polymer chains, thereby resulting in an incremental increase in the T_g value.[15] There are two major causes to the reduction in the mobility of polymer chains in composites i.e., tethering and chain confinement.[14,15] The chain tethering is caused by the attractive forces between the filler surfaces and polymer chains. On the other hand, the chain confinement occurs when the mobility of polymer chains is significantly obstructed by the fillers. The T_g values of 35.1 mol % and higher concentration ZnO/PI slightly increased because of the chain confinement because there was little attractive force between the surface of ZnO and polymer chains.[14] By the way, T_g was not observed in the DSC thermographs of Zn nitrate/PI (data not shown). It could be ascribed to the formation of ZnO[12,13] during the combined decomposition and imidization of $Zn(NO_3)_2$/PI films. The brittleness of the film may be due to the chain scission caused by generated nitric acid or ions. In addition, the formation of ZnO may affect the mobility of polymer chain, which is reflected to the obscured glass transition in $Zn(NO_3)_2$/PI film.

The presence of ZnO nanoparticles in PI films also affected their degradation temperature (T_d), which is defined as the temperature of the samples at 5 wt % loss. It was found that the T_d of $Zn(NO_3)_2$/PI are lower than those of ZnO/PI. Figure 4 showed typical thermogravimetric profiles of $Zn(NO_3)_2$/PI films. As shown in Table I, the addition of only 5 mol % of $Zn(NO_3)_2$ into PI decreased the T_d by 17°C. However, adding more amounts of $Zn(NO_3)_2$/PI from 5 to 117.6 mol % dramatically decrease the T_d by 17 to 204°C. Figure 5 shows typical thermogravimetric profiles of ZnO/PI films. The T_d of these nanocomposites clearly decrease to a certain extent when adding ZnO nanoparticles directly into the films, as shown in Table I. Addition of 0.6–117.6 mol % of ZnO into PI films decreases the T_d by 20–50°C. Interestingly, the ZnO/PI and $Zn(NO_3)_2$/PI films prepared at the same 35.1 mol % concentration show different thermogravimetric profiles. The T_d of ZnO/PI decrease only by 35°C compared to 132°C in the case of $Zn(NO_3)_2$/PI. Obviously the ZnO/PI film has better thermal stability than the $Zn(NO_3)_2$/PI film. The difference between the T_d of ZnO/PI and that of $Zn(NO_3)_2$/PI film was a consequence of the origin of ZnO nanoparticles. Since metallic salts added into PI films induced acidic hydrolysis (chain scission) and oxidative degradation of polyimide,[12,13] the T_d of $Zn(NO_3)_2$/PI film decreased dramatically. This result was consistent with Hsu et al.'s [10] and Chiang and Whang's.[13]

TABLE 1
The Degradation Temperature of Pure PI, ZnO/PI and Zn Nitrate/PI

ZnO content (mol %)	Zn nitrate/PI		ZnO/PI	
	T_d (°C)	ΔT_d (°C)	T_d (°C)	ΔT_d (°C)
Pure PI	555	–	555	–
0.6	–	–	535	−20
3.3	–	–	523	−32
5	538	−17	–	–
10	494	−61	–	–
15	484	−71	–	–
35.1	423	−132	520	−35
74.1	399	−156	508	−47
117.6	351	−204	505	−50

T_d was defined as T of material at 5 wt % loss.
$\Delta T_d = T_d - T_d$ (pure PI).

The optical absorbance and fluorescence spectra observed for the PI films containing 35.1 mol % ZnO

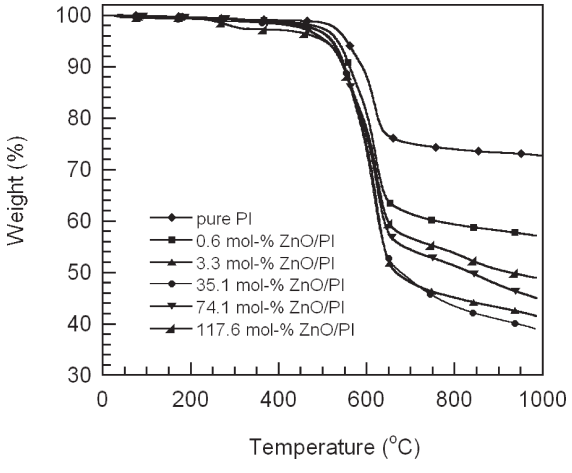

Figure 5 Thermogravimetric profiles of PI containing directly added ZnO nanoparticles.

ID: 40410 Date: 15/4/08 Time: 17:56 Path: J:/Production/APP#/Vol00000/080384/3B2/C2APP#080384

J_ID: Z8E Customer A_ID: APP28299 Date: 15-APRIL-08 Stage: I Page: 5

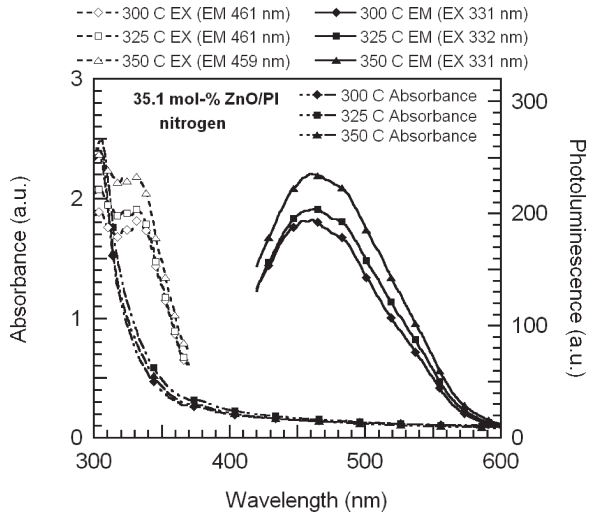

Figure 6 Effect of curing temperature on fluorescence of 35.1 mol % ZnO/PI cured under nitrogen atmosphere.

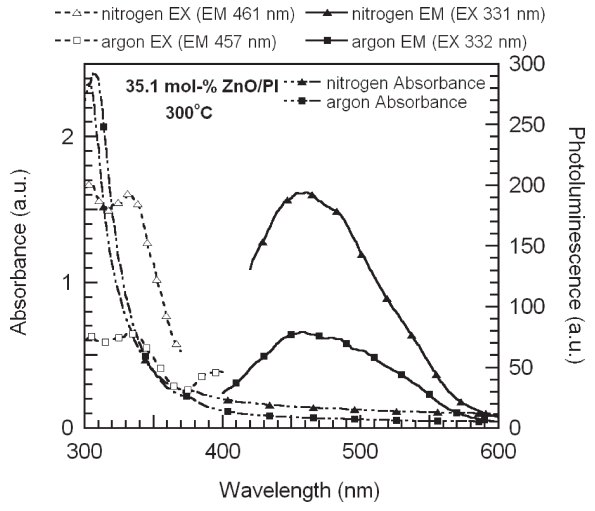

Figure 7 Effect of curing atmosphere on fluorescence of 35.1 mol % ZnO/PI cured at 300°C.

at different curing temperatures are shown in Figure 6. The characteristic peaks attributable to the exciton absorption of ZnO are observed at 305 nm for all the ZnO/PI films with different curing temperatures. The absorption spectra of all films are shown in the range of 305–410 nm, and the absorption was quenched above 410 nm. The emission peak of all films was located at 461 nm for both 300°C and 325°C curing temperatures and was slightly shifted to 469 nm for the film cured at 350°C. The intensity of emission slightly increased as the curing temperature increased. Though the data are not shown here, the effect of the curing temperature at a different fixed ZnO concentration exhibited a similar trend as the one just mentioned. Since the effect of curing temperature on the fluorescent intensity is slight, the curing temperature of 300°C was chosen to explore the effect on fluorescence.

Figure 7 shows the effects of curing atmosphere, nitrogen or argon, on the absorbance and fluorescence at room temperature of 35.1 mol % ZnO/PI films. The films were imidized at 300°C under either nitrogen or argon atmosphere. The exciton absorption peaks of the films cured under nitrogen and argon atmosphere are observed at 302 and 307 nm, respectively. The film prepared under nitrogen shows emission and excitation peaks at 461 and 331 nm, respectively. Similarly the film prepared under argon showed peaks at 457 and 332 nm, respectively. The emission peak of the former is slightly red shifted and exhibited 2.4 times higher intensity than the latter which is consistent with Roy et al.[16] ZnO synthesized under nitrogen emitted higher intensity of green light than that prepared under argon which could be due to different intrinsic defects in ZnO such as oxygen vacancy and interstitial zinc. The effect of the curing atmosphere at other ZnO concentrations exhibited similar trends (the spectra are not shown here).

The effects of ZnO concentration on the fluorescence and absorbance were presented in Figures 8–11. All the films were imidized at 300°C under nitrogen. As expected, the existence of ZnO in PI films enhanced the fluorescence emission. Figures 8 and 9 show the effect of ZnO/PI concentration on the optical absorption and emission intensity, respectively. As the concentration of ZnO nanoparticles increases from 0.6 to 117.6 mol %, Figure 8 shows that the exciton absorption peak is blue shifted from 318 to 295 nm and the absorbance decreased. This phenomenon is caused by the broadened distribution of aggregates of ZnO nanoparticles in the PI film, which was confirmed by TEM image (Fig. 13). All samples exhibited absorption spectra in the range of 300–370 nm. Above 370 nm, the absorbance of pure

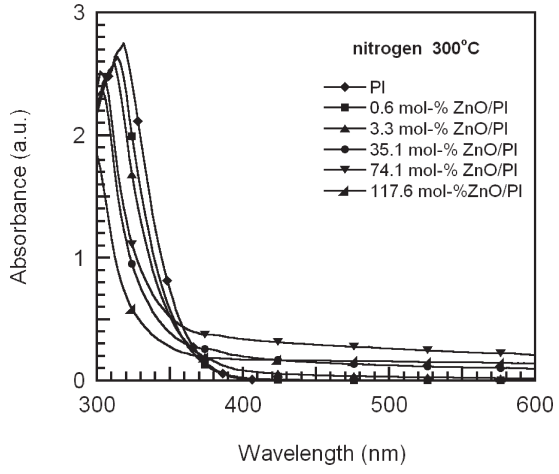

Figure 8 Effect of ZnO concentration on absorbance of ZnO/PI cured under nitrogen atmosphere at 300°C.

ID: 40410 Date: 15/4/08 Time: 17:56 Path: J:/Production/APP#/Vol00000/080384/3B2/C2APP#080384

J_ID: Z8E Customer A_ID: APP28299 Date: 15-APRIL-08 Stage: I Page: 6

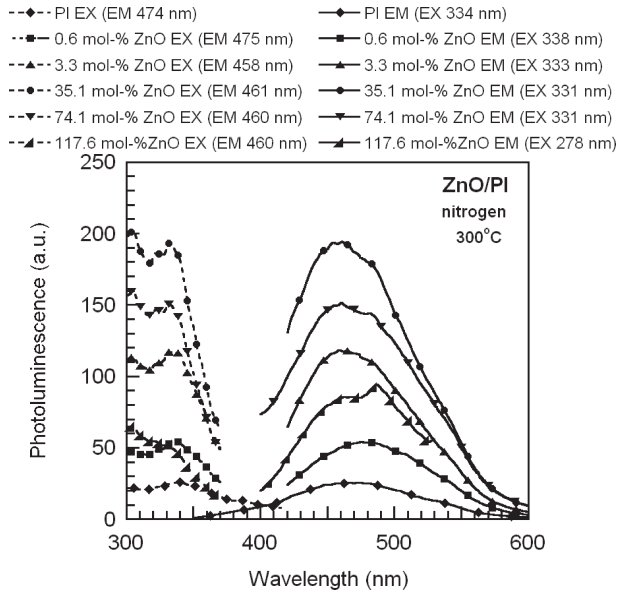

Figure 9 Effect of ZnO concentration on fluorescence of ZnO/PI cured under nitrogen atmosphere at 300°C.

PI, 0.6 and 3.3 mol % ZnO/PI films was quenched in the visible region. However, some incremental absorbance intensity in the visible region (above 370 nm) was detected in high-concentration ZnO/PI films (>35.1 mol % ZnO) due to the presence of submicron-size ZnO particles, which was confirmed by TEM micrograph (Fig. 13). The high-concentration ZnO/PI films are less transparent than the corresponding $Zn(NO_3)_2$/PI films because submicron-sized ZnO cause significant light scattering in the visible region.

Figure 9 shows that, as the concentration of ZnO nanoparticles increased to 3.3 mol %, the fluorescent intensity increased and was slightly blue shifted from 474 to 458 nm compared to that of pure PI, although the wavelength of the excitation peak of all films was approximately the same (except the case of 117.6 mol % ZnO). As the concentration of ZnO nanoparticles increased to 35.1 mol % and above, the fluorescent intensity is, however, not shifted further compared to that of 3.3 mol % ZnO/PI. More specifically, at 0.6 and 35.1 mol % of ZnO nanoparticles, the fluorescent intensity at visible wavelength was enhanced by 2.2 and 7.8 times compared to that of pure PI. However, adding more amounts of ZnO nanoparticles at 74.1 and 117.6 mol % to the films, the light emission intensity was dramatically decreased because of the self-absorption of ZnO. Fluorescence was generally inversely proportional to the concentration owing to the concentration quenching,[17] which can be classified into two categories: self-quenching and self-absorption. Self-quenching is a collision phenomenon between molecules in the ground state and those in excited state conditions, which leads to the energy transfer without fluorescence. On the other hand, self-absorption is a phenomenon in which the wavelength of fluorescence overlaps that of the absorption by the sample. In other words, the fluorescence was absorbed by the other molecules. This is consistent with the appearance of an increase in the absorption in the visible region (above 370 nm). Moreover, the emission in the visible region at all concentrations of ZnO nanoparticles except 0.6 mol % in PI films showed two main peaks at 460 and 485 nm, similar to the result by Roy et al.[16] The peak appearing at 485 nm could be originated from oxygen vacancy defect in ZnO.

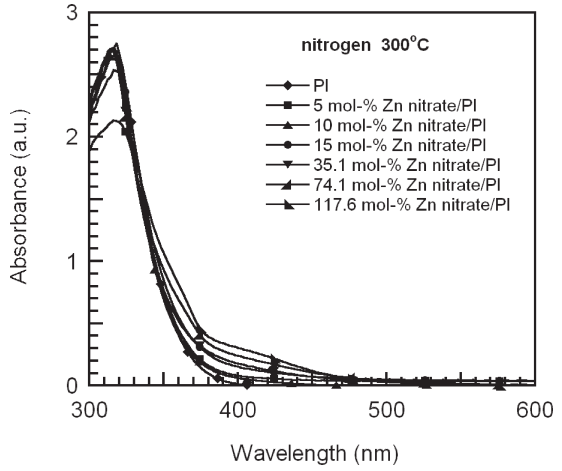

Figure 10 Effect of ZnO concentration on absorbance of Zn nitrate/PI cured under nitrogen atmosphere at 300°C.

Similarly, the effects of ZnO concentration from thermal decomposition of $Zn(NO_3)_2$ in PI films on the absorbance and fluorescence of Zn nitrate/PI films were shown in Figures 10 and 11, respectively.

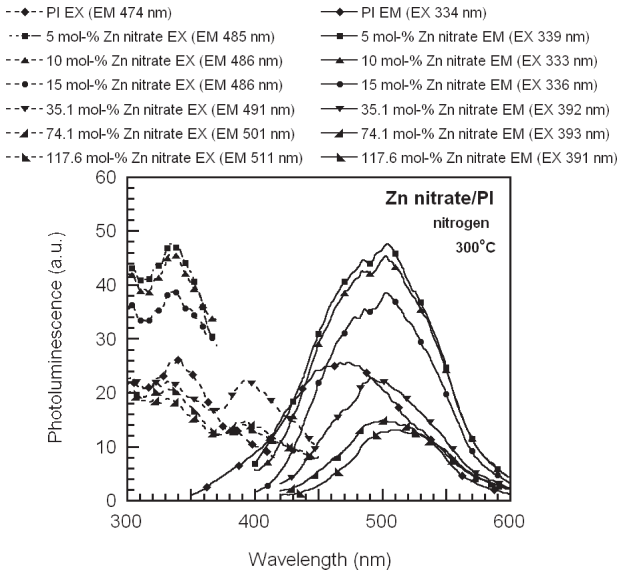

Figure 11 Effect of ZnO concentration on fluorescence of Zn nitrate/PI cured under nitrogen atmosphere at 300°C.

ID: 40410 Date: 15/4/08 Time: 17:56 Path: J:/Production/APP#/Vol00000/080384/3B2/C2APP#080384

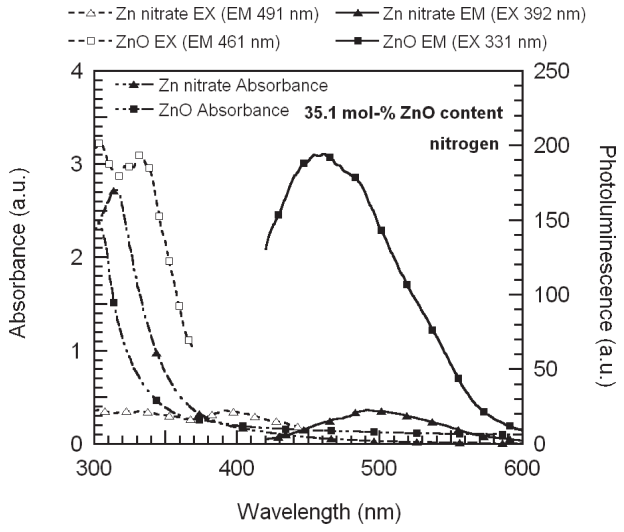

Figure 12 Effect of the origin of ZnO at concentration of 35.1 mol % on fluorescence cured under nitrogen atmosphere at 300°C.

In Figure 10, $Zn(NO_3)_2$/PI films of all concentrations exhibit broad absorption in the range of 300–370 nm with peaks around 318 nm. The absorption above 370 nm gradually increase as the concentration of $Zn(NO_3)_2$ increase due to the increase in particle size of ZnO as confirmed by XRD. However, the exciton absorption peak at all Zn nitrate concentrations was not shifted compared to that of the ZnO/PI films.

Figure 11 showed the effect of ZnO concentration in $Zn(NO_3)_2$/PI films on the fluorescent intensity and wavelength. Adding only 5 mol % of $Zn(NO_3)_2$ to the PI film shows the highest intensity in the visible region compared to all other concentrations. In fact, the fluorescent intensity of 5 mol % Zn nitrate/PI was 1.9 times that of the pure PI. On the other hand, the intensities of 10 and 15 mol % Zn $(NO_3)_2$/PI are lower than that of 5 mol % $Zn(NO_3)_2$/PI, whereas the fluorescent intensity of 35.1, 74.1, and 117.6 mol % $Zn(NO_3)_2$/PI films became even lower than that of pure PI as the concentration increases owing to the aggregation of ZnO nanoparticles. Moreover, the emission peak of these $Zn(NO_3)_2$/PI films was red shifted when compared to that of the pure PI films, which may also be attributed to the aggregation of ZnO nanoparticles. This result is consistent with the appearance of the increasing absorption above 370 nm. In contrast, the light emission of ZnO/PI was slightly blue shifted because of no change in the size of ZnO nanoparticles in the PI films, which was confirmed by TEM image (Fig. 13).

By the way, the visible light emission of 5, 10, and 15 mol % $Zn(NO_3)_2$/PI showed two main peaks at 486 and 502 nm, similar to the results reported by Roy et al.[16] In addition, all samples emitted green color. The visible light emission was assumed to be caused by different intrinsic defects in ZnO such as oxygen vacancy and interstitial zinc (450–600 nm).[18–20]

Figure 12 showed the effect of the origin of ZnO F12
on the absorbance and fluorescence of PI films at the same ZnO concentration of 35.1 mol %. The films were imidized at 300°C under nitrogen. The exciton absorption peaks of $Zn(NO_3)_2$/PI and ZnO/PI are observed at 313 and 301 nm, respectively. Both PI films show absorption bands in the range of 300–400 nm. However, an increase in absorbance (above 400 nm) was observed for ZnO/PI compared to that of $Zn(NO_3)_2$/PI. Furthermore, the fluorescence of ZnO/PI shows an emission peak at 461 nm, which is significantly blue shifted from the 491 nm of $Zn(NO_3)_2$/PI, and also exhibits a much higher intensity. The excitation and emission peaks of ZnO/PI are enhanced by 8.7 times than those of $Zn(NO_3)_2$/

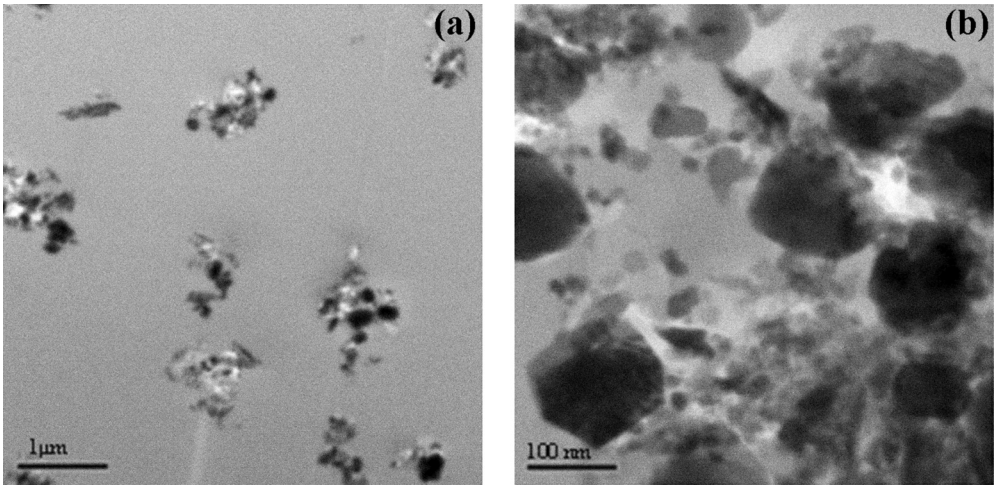

Figure 13 TEM images of polyimide containing 117.6 mol % ZnO nanoparticles (a) low magnification image (×12,000) (b) high magnification image (×120,000).

J_ID: Z8E Customer A_ID: APP28299 Date: 15-APRIL-08 Stage: I Page: 8

PI, which is attributed to an imperfect crystal structure and smaller crystallite sizes of ZnO nanoparticles in $Zn(NO_3)_2$/PI films (confirmed with XRD data). In addition, the ZnO generated from the thermal decomposition of $Zn(NO_3)_2$ in PI films results in more self-quenching than ZnO nanoparticles dispersed in ZnO/PI films.

The TEM images of 117.6 mol % ZnO/PI films are shown in Figure 13(a,b). Obviously the ZnO nanoparticles are well distributed throughout the film but poorly dispersed in PI films as can be seen in Figure 13(a). The diameter of ZnO primary particle obtained from the vendor is around 2 nm. The aggregates of ZnO nanoparticles with an average diameter of 17–90 nm are observed in Figure 13(b) and approximately agglomeration of ZnO nanoparticles with average size of 114–150 nm is also observed. However, small ZnO nanoparticles generated from the thermal decomposition of $Zn(NO_3)_2$ are not observed in this study mainly due to the limitation of TEM resolution capacity (data not shown).

CONCLUSIONS

The thermal conversion of zinc nitrate hexahydrate ($Zn(NO_3)_2{\cdot}6H_2O$) to zinc oxide (ZnO) nanoparticles was confirmed by XRD technique. The glass transition temperature (T_g) of ZnO nano-particle-dispersed polyimide films (ZnO/PI) slightly increase when the concentration of ZnO nanoparticles is higher than 35.1 mol %, which is due to the confinement of polymer chain mobility by ZnO. However, no T_g of $Zn(NO_3)_2$/PI were observed in the film. The 5 wt % degradation temperatures (T_d) of all nanocomposite films are lower than that of pure PI, though the ZnO/PI films exhibits higher thermal stability than $Zn(NO_3)_2$/PI films.

The 35.1 mol % ZnO/PI exhibits fluorescence with the highest intensity, which is 7.8 times as high as that of pure PI. In fact, the fluorescent intensities of all ZnO/PI films are higher than that of pure PI. An addition of only 5 mol % $Zn(NO_3)_2$ enhances the fluorescence by 1.9 times compared with that of pure PI. Moreover, the light emission of $Zn(NO_3)_2$/PI films shows a red shift compared to that of pure PI. This may be attributed to the aggregation of ZnO nanoparticles. As for the effect of the curing atmosphere on fluorescence, the films prepared under nitrogen emit higher fluorescent intensity than those prepared under argon. However, the curing temperature gives slightly effect on the fluorescent intensity. The TEM images show ZnO nanoparticles embedded in PI films in which the aggregates with an average diameter of 17–90 nm are observed. In addition, ZnO nanoparticles agglomerate with average size of 114–150 nm. In other words, ZnO nanoparticles are well distributed but poorly dispersed in the PI films. It is expected that the optical properties of the ZnO-containing PI films would be further enhanced if the ZnO nanoparticles could be uniformly distributed and dispersed as primary particles in the films.

The authors thank Dr. Toemsak Srikhirin, Department of Physics, Faculty of Science, Mahidol University for use of luminescence spectrometer and spectrophotometer for this study.

References

1. Ghosh, M. K.; Mittal, K. L. Polyimides Foundamentals and Applications; Marcel Dekker: New York, 1996.
2. Chiron, D.; Trigaud, T.; Moliton, J. P. Synthetic Met 2001, 124, 33.
3. Cornic, C.; Lucas, B.; Moliton, A.; Colombeau, B.; Mercier, R. Synthetic Met 2002, 127, 299.
4. Kim, J. H.; Koros, W. J.; Paul, D. R. Polymer 2006, 47, 3104.
5. Kim, H.; Horwitz, J. S.; Kim, W. H.; Mäkinen, A. J.; Kafafi, Z. H.; Chrisey, D. B. Thin Solid Films 2002, 539, 420.
6. Cembrero, J.; Elmanouni, A.; Hartiti, B.; Mollar, M.; Mari, B. Thin Solid Films 2004, 198, 451
7. Hirai, T.; Harada, Y.; Hashimoto, S.; Itoh, T.; Ohno, N. J lumin 2004, 112, 196.
8. Tsukazaki, A.; Ohtomo, A.; Onuma, T.; Ohtani, M.; Makino, T.; Sumiya, M.; Ohtani, K.; Chichibu, S. F.; Fuke, S.; Segawa, Y.; Ohno, H.; Koinuma, H.; Kawasaki, M. Nat Mater 2005, 4, 42.
9. Guo, L.; Yang, S.; Yang, C.; Yu, P.; Wang, J.; Ge, W.; Wong, G. K. L. Chem Mater 2003, 12, 2268.
10. Hsu, S. C.; Whang, W. T.; Hung, C. H.; Chiang, P. C.; Hsiao, Y. N. Macromol Chem Phys 2005, 206, 291.
11. Andelman, T.; Gong, Y.; Polking, M.; Yin, M.; Kuskovsky, I.; Neumark, G.; O'Brien, S. J Phys Chem B 2005, 109, 14314.
12. Sawada, T.; Ando, S. Chem Mater 1998, 10, 3368.
13. Chiang, P. C.; Whang, W. T. Polymer 2003, 44, 2249.
14. Chae, D. W.; Kim, B. C. Polym Adv Technol 2005, 16, 846.
15. Savin, D. A.; Pyun, J.; Patterson, G. D.; Kowalewski, T.; Matyjaszewski, K. J Polym Sci Pol Phys 2002, 40, 2667.
16. Roy, V. A. L.; Djurisic, A. B.; Chan, W. K.; Gao, J.; Lui, H. F.; Surya, C. Appl Phys Lett 2003, 83, 141.
17. Lawan, S. Fluorometric analysis; Faculty of Pharmaceutical Sciences Sillapakron University: Nakonpatom, 2544.
18. Lin, B.; Fu, Z.; Jia, Y. Appl Phys Lett 2001, 79, 943.
19. Lin, Y.; Xie, J.; Wang, H.; Li, Y.; Chavez, C.; Lee, S. Y.; Foltyn, S. R.; Crooker, S. A.; Burrell, A. K.; McCleskey, T. M.; Jia, Q. X. Thin Solid Films 2005, 492, 101.
20. Masuda, Y.; Kinoshita, N.; Sato, F.; Koumoto, K. Cryst Growth Des 2006, 6, 75.

ID: 40410 Date: 15/4/08 Time: 17:56 Path: J:/Production/APP#/Vol00000/080384/3B2/C2APP#080384

AQ1: Kindly check whether the short title is OK as given.

AQ2: Please provide the full details of this reference so as to help a reader locate this reference.